University of Maribor
Faculty of Energy Technology

Journal of ENERGY TECHNOLOGY

Volume 9 / Issue 4
DECEMBER 2016
www.fe.um.si/en/jet.html

Journal of
ENERGY TECHNOLOGY

VOLUME 9 / Issue 4

Revija Journal of Energy Technology (JET) je indeksirana v bazah INSPEC© in Proquest's Technology Research Database.

The Journal of Energy Technology (JET) is indexed and abstracted in database INSPEC© and Proquest's Technology Research Database.

JOURNAL OF ENERGY TECHNOLOGY

Ustanovitelj / FOUNDER

Fakulteta za energetiko, UNIVERZA V MARIBORU /
FACULTY OF ENERGY TECHNOLOGY, UNIVERSITY OF MARIBOR

Izdajatelj / PUBLISHER

Fakulteta za energetiko, UNIVERZA V MARIBORU /
FACULTY OF ENERGY TECHNOLOGY, UNIVERSITY OF MARIBOR

Tehnični urednik / TECHNICAL EDITOR

Sonja Novak

Tehnična podpora / TECHNICAL SUPPORT

Tamara BREČKO BOGOVČIČ

Izhajanje revije / PUBLISHING

Revija izhaja štirikrat letno v nakladi 150 izvodov. Članki so dostopni na spletni strani revije - www.fe.um.si/si/jet.html / The journal is published four times a year. Articles are available at the journal's home page - www.fe.um.si/en/jet.html.
Cena posameznega izvoda revije (brez DDV) / Price per issue (VAT not included in price): 50,00 EUR
Informacije o naročninah / Subscription information: http://www.fe.um.si/en/jet/subscriptions.html

Lektoriranje / LANGUAGE EDITING

Terry T. JACKSON

Oblikovanje in tisk / DESIGN AND PRINT

Fotografika, Boštjan Colarič s.p.

Naslovna fotografija / COVER PHOTOGRAPH

Jurij AVSEC

Oblikovanje znaka revije / JOURNAL AND LOGO DESIGN

Andrej PREDIN

Ustanovni urednik / FOUNDING EDITOR

Andrej PREDIN

Izdajanje revije JET finančno podpira Javna agencija za raziskovalno dejavnost Republike Slovenije iz sredstev državnega proračuna iz naslova razpisa za sofinanciranje domačih znanstvenih periodičnih publikacij / The Journal of Energy Technology is co-financed by the Slovenian Research Agency.

Spoštovani bralci revije Journal of energy technology (JET)

Število ljudi na planetu Zemlja naglo narašča. Projekcije kažejo, da naj bi bilo okoli leta 2100 na planetu približno 12 milijard ljudi. Ekološka problematika, raziskave na področju ekologije in varovanje naravnega okolja bodo zelo pomembni segmenti v energetiki. Da bomo lahko preživeli in ohranili zdravo okolje, bo potrebno še v večji meri uporabljati obnovljive vire. Hkrati bo potrebno uporabljati tehnologije, ki manj škodljivo vplivajo na okolje. Takšen primer je npr. tudi postopek čiščenja dimnih plinov. Sodobne termoelektrarne si prizadevajo zmanjšati obremenitev okolja z vgradnjo sistemov za razžvepljevanje plinov, zmanjšanje emisij dušikovih oksidov in odstranitev prašnih delcev. Takšno tehnologijo uporabljajo že dobra tri desetletja tudi v Termoelektrarni Šoštanj. Po uporabi mokrega kalcitnega postopka za razžvepljevanje dimnih plinov se je kvaliteta zraka v Šaleški dolini občutno izboljšala. Problematika kvalitete zraka v slovenskih mestih je izjemno pomembna; na tem področju nas čaka v bližnji prihodnosti še veliko dela. Tematiko povezano s čiščenjem dimnih plinov lahko najdemo tudi v tej številki revije.

Jurij AVSEC
odgovorni urednik revije JET

Dear Readers of the Journal of Energy Technology (JET)

The population of planet Earth is increasing rapidly. Projections show that about 12 billion people will be on the planet around the year 2100. Ecological issues, research in the field of ecology, and protection of the natural environment will be a vital part of the energy sector in the near future. In order to survive and maintain a healthy environment, renewable sources will be used to an even greater extent. At the same time, it will be necessary to use technologies that are less harmful to the environment, such as the process for the purification of flue gases. Modern thermal power plants strive to reduce the burden on the environment by the installation of desulphurization of gases, reduction of emissions of nitrogen oxides, and removal of dust particles. Such technology has been used for more than three decades in the Šoštanj Thermal Power Plant. After using the wet calcite process for flue gas desulphurisation, the air quality in the Šalek valley greatly improved. The issue of air quality in Slovenian cities is crucial; much work in this field awaits us in the near future. Themes associated with the cleaning of flue gases can also be found in this issue of JET.

Jurij AVSEC
Editor-in-chief of JET

Table of Contents / Kazalo

Journal of Energy Technology

JET Volume 9 (2016) p.p. 11-20
Issue 4, December 2016
Type of article 1.01
www.fe.um.si/en/jet.html

PRINCIPLES OF WATER HAMMER INTERFEROMETER

OSNOVE VODNO UDARNEGA INTERFEROMETRA

Anton Bergant[ℜ]

Keywords: pipeline, two-valve system, control, water hammer, interference

Abstract

This paper presents a novel water hammer interferometer. In essence, it is an acoustic tube interferometer using the controlled closure of two valves. The device generates two water hammer waves that interfere with each other along the liquid-filled pipeline. The superposition of the two waves can generate pressure head variations of different frequencies and amplitudes. The frequency and shape of pressure histories are controlled via the delayed closure of one of the two valves. The interference phenomena in an ideal pipeline system are described with the aid of basic water hammer theory.

Povzetek

Prispevek obravnava nov vodno udarni interferometer. V osnovi je to akustični cevni interferometer, ki je krmiljen z zapiranjem dveh ventilov. Naprava generira dva vodno udarna vala, ki medsebojno delujeta vzdolž s kapljevino napolnjene cevi. Superpozicija teh dveh valov lahko generira oscilacije tlačnih višin različnih frekvenc in amplitud. Frekvenca in oblika tlačnih valov sta krmiljeni s časovnim zamikom zapiranja enega od dveh ventilov. Interferenčni pojavi v idealnem cevnem sistemu so popisani s pomočjo osnovne teorije vodnega udara.

[ℜ] Corresponding author: Anton Bergant, PhD, Litostroj Power d.o.o., Litostrojska 50, 1000 Ljubljana, Slovenia, anton.bergant@litostrojpower.eu

1 INTRODUCTION

Liquid-filled pipelines in energy systems undergo a broad range of operating regimes (valve closure, pump failure, turbine shutdown). Unsteady pipe flows may induce large pressure pulsations and pipeline vibrations. Water hammer is the propagation of pressure waves along liquid-filled pipelines (water, oil), and it is induced by a change in flow rate (flow velocity). Most of the water hammer research has been done for a standard case with single-valve closure in a simple reservoir-pipeline-valve system, *[1]*, *[2]*. However, there are a number of typical industrial pipelines with multiple valves, at least with two of them (upstream- and downstream-end valves). Multiple closing or opening of valves may induce very large or low-pressure waves due to the superposition of the waves, *[3]*, *[4]*.

This paper further investigates the effects of multiple-valve closure (closure of upstream-end and downstream-end valves). The system under consideration is a simple reservoir-valve-pipeline-valve system (two-valve system). The two valves can be closed either simultaneously, or one is shut with a time delay. This may produce large or very low pressures depending on the valve control scenario, *[4]*, *[5]*. Naturally, the different position of two valves may also play a major role, *[6]*, but this is not the subject of this paper. The two valves are positioned at the two far ends. In essence, the system with two closing far-end valves generates two water hammer waves that superimpose at some point along the pipeline. This causes interference from the physical effects of superimposing two waves, *[7]*. The superposition of waves can generate a wave of greater, lower or the same amplitude. More strictly, interference refers to the interaction of waves that are correlated or coherent with each other, *[8]*. In nature, interference effects can be observed with all types of waves, including acoustic waves (for example our case study with pressure waves in closed conduit), surface water waves, light waves, etc. In 1833, Herschel first developed an idea of acoustic interference, *[9]*. Then in 1866 Quincke, *[10]*, experimentally proved Herschel's cancellation of acoustic waves. This lead to the development of the Herschel-Quincke tube that is, in essence, a bypass pipe connected to the main pipeline. Pressure pulsations in the pipeline are controlled by the right relation between the length of the main pipe between T-junctions and the length of the by-pass line.

The concept of a proposed acoustic tube interferometer using the controlled action of two valves is new. Because the two waves are water hammer waves, the device is called *water hammer interferometer*. This paper first presents the basic water hammer theory that is used for the detailed description of the interferometer in the core of the paper.

2 BASIC WATER HAMMER THEORY

The water hammer phenomenon is traditionally explained by considering an ideal reservoir-pipe-valve system (frictionless) in which a steady flow with velocity V_0 is stopped by an instantaneous valve closure (see Fig. 1). The valve closure generates a pressure wave that travels at the wave speed, a, towards the reservoir at a distance, L. The pressure rise, Δp, induced by the pressure wave is given by the Joukowsky formula, *[1], [2]*:

$$\Delta p = \rho a V_0 \tag{2.1}$$

where ρ is the mass density of the fluid. Herein it is assumed that pressure never drops below the liquid vapour pressure during a water hammer event.

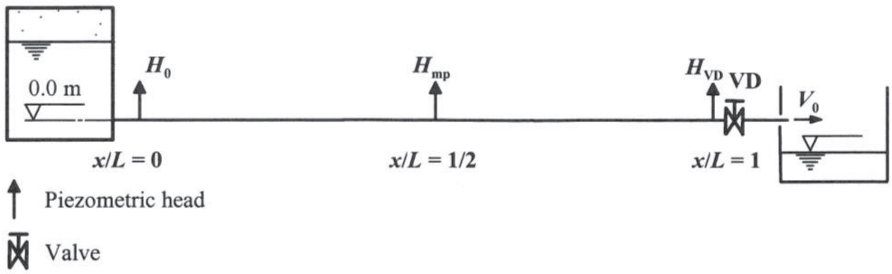

Figure 1: *Reservoir-pipe-valve system*

In the hydropower and pump industries, the pressure p is replaced by the piezometric head (pressure head) H ($H = p/(\rho g)$) and flow velocity V_0 with velocity amplitude $\Delta V = 0 - V_0 = - V_0$; then Eq. (2.1) may be written as

$$\Delta H = -\frac{a}{g}\Delta V \tag{2.2}$$

Pressure waves in the ideal system are plane waves, and the resulting pressure head traces are obtained from Eq. (2.2). For a valve closure event in a simple reservoir-pipe-valve system, there are two basic dimensionless numbers, *[1]*: (1) dimensionless pressure (pressure head change divided by Joukowsky head rise: $(H\text{-}H_0)/((a/g)V_0)$ in our case) and (2) dimensionless time (time divided by wave reflection time: $t/(L/a)$). Pressure head waves in the ideal system of Fig. 1 at the downstream end (x/L = 1), at the midpoint (x/L = 1/2) and at the upstream end of the pipe system (x/L = 0) are presented in a dimensionless form in Fig. 2.

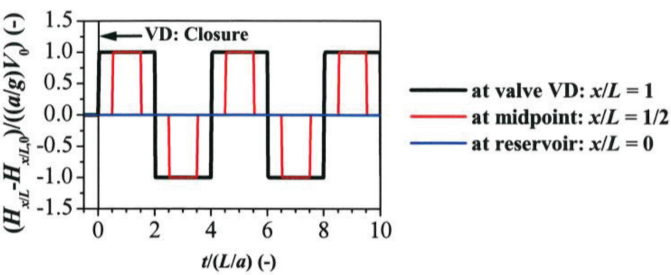

Figure 2: Dimensionless pressure head histories in the ideal reservoir-pipe-valve system: Instantaneous closure of the downstream end valve VD

The complete period resulting from an instantaneous valve closure in this open-closed system is $4L/a$ (Fig. 2). The corresponding natural frequency of the vibration is $a/(4L)$. The phenomenon can be described as follows:

1) $0 < t \leq L/a$: After instantaneous valve closure, the high-pressure head wave $+\Delta H$ ($H-H_0 = (a/g)V_0$) travels towards the upstream end reservoir at a wave speed a. At time L/a, all the liquid is brought to rest, and the wave reflects off the constant head reservoir.

2) $L/a < t \leq 2L/a$: The reflected negative wave $-\Delta H$ travels back to the downstream end valve. At time $2L/a$ all the liquid has a velocity $-V_0$ (reverse velocity) and the wave reflects off the closed valve as a negative wave $-\Delta H$.
3) $2L/a < t \leq 3L/a$: The low-pressure head wave $-\Delta H$ travels towards the reservoir. At time $3L/a$ all the liquid in the pipe is brought to rest, and the wave reflects off the reservoir as positive wave $+\Delta H$.
4) $3L/a < t \leq 4L/a$: The $+\Delta H$-wave travels back to the closed downstream end valve (dead end). At time 4L/a, all the liquid in the pipe has a velocity $+V_0$. At this instant, the conditions are the same as at the instant of the instantaneous closure.

The time interval of 4L/a is termed the theoretical period of the pipeline, *[2].* The pressure head variations repeat forever; however, in reality, the pressure head variations will die out because of skin friction and other damping mechanisms *[11]*, *[12]*.

3 WATER HAMMER INTERFEROMETER PRINCIPLES

The proposed water hammer interferometer is comprised of an upstream end constant-head reservoir, a valve positioned adjacent to the reservoir (valve VU), pipeline, and a downstream end valve (valve VD) (see Fig. 3). Water hammer waves are induced by the closure of the two valves (valves VU and VD) either simultaneously, or one of them shuts with delay (either VU or VD). The reservoir is the source of energy. Let us consider an ideal frictionless system and instantaneous valve closure for the easiest visualization of the two pressure head (water hammer) waves. Then water hammer phenomena can be explained by the simple relations presented in Section 2. Transient phenomena are investigated by comparing the responses of an ideal standard reservoir-pipe-valve system (Section 2) and an ideal water hammer interferometer (reservoir-valve-pipe-valve system). Pressure head traces are depicted in a dimensionless form at the downstream end (x/L = 1), at the midpoint (x/L = 1/2) and at the upstream end of the pipe system. Dimensionless head traces are the same for any similar pipeline system. Results are presented for the case of simultaneous valve closure and for the case of delayed closure of the upstream end valve VU (time delay: $0 < t_{d,VU} \leq 4L/a$). Flow situations with the delayed closure of the downstream end valve VD are more complex. In the ideal system, the wave phenomena are similar to the case with the delayed closure of the valve VU when (1) the valve VD shuts with a delay less than L/a or (2) a second constant-head reservoir is simply attached to the downstream end. Wave phenomena in systems with two acting valves positioned at an arbitrary location along the pipeline are even more complex and require detailed transient analysis, *[1]*, *[2].*

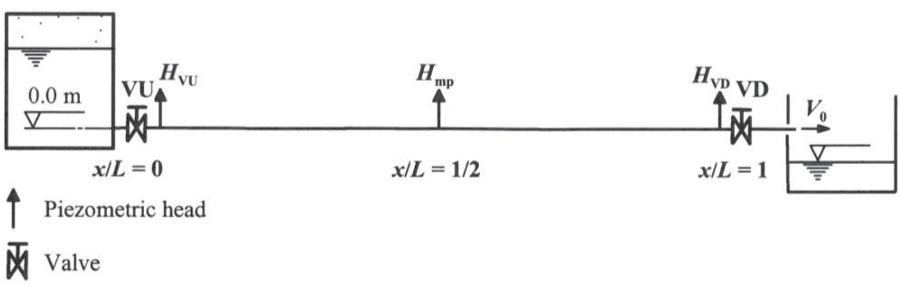

Figure 3: Reservoir-valve-pipe-valve system

Figure 4 presents pressure head response for the case of simultaneous valve closure and for the case of delayed closure of the upstream end valve VU with a time delay from 0 to $2L/a$. The time period of $2L/a$ is actually the round-trip wave travel time. Figure 4a repeats pressure head response in the conventional reservoir-pipe-valve system that is well explained in Section 2. The theoretical period of head variations is $4L/a$, and it is equal to the theoretical period of the pipeline (Section 2).

The flow situation for the two-valve closure case is more complex. Simultaneous valve closure (Fig. 4b) produces pressure head variations at the two far end valves with a period of $2L/a$, whereas the head at the midpoint remains constant at all times. In this case, interference of the two water hammer waves produces waves of different frequencies and cancellation of waves in comparison to the case of single-valve closure (Fig. 4a). The delayed closure of the upstream end valve VU at the time of $0.5L/a$ and at $1.5L/a$ after VD closure shows a similar response (Figs. 4c and 4e). In this case, pressure heads at the two far end valves vary with a period of $2L/a$, whereas the pressure head at the midpoint exhibits variation in the period of L/a. Pressure head in the midpoint never drops below the initial static head. Even more striking is the response of the second valve closure (VU) at time L/a after the first valve closure (VD; Fig. 4d). The interference of two water hammer waves completely cancels the pressure variations at the two valves and at the midpoint. Moreover, the pressure head is increased by the Joukowsky pressure head rise of $(a/g)V_0$. The interferometer works as a pressure head amplifier. The flow situation induced by the second valve closure (VU) at time $2L/a$ after the first valve closure (VD; Fig. 4f) is in a way similar to the situation of simultaneous valve closure (Fig. 4b). Wave interference produces pressure head variations at the two far end valves with a period of $2L/a$, whereas the head at the midpoint remains constant at all times.

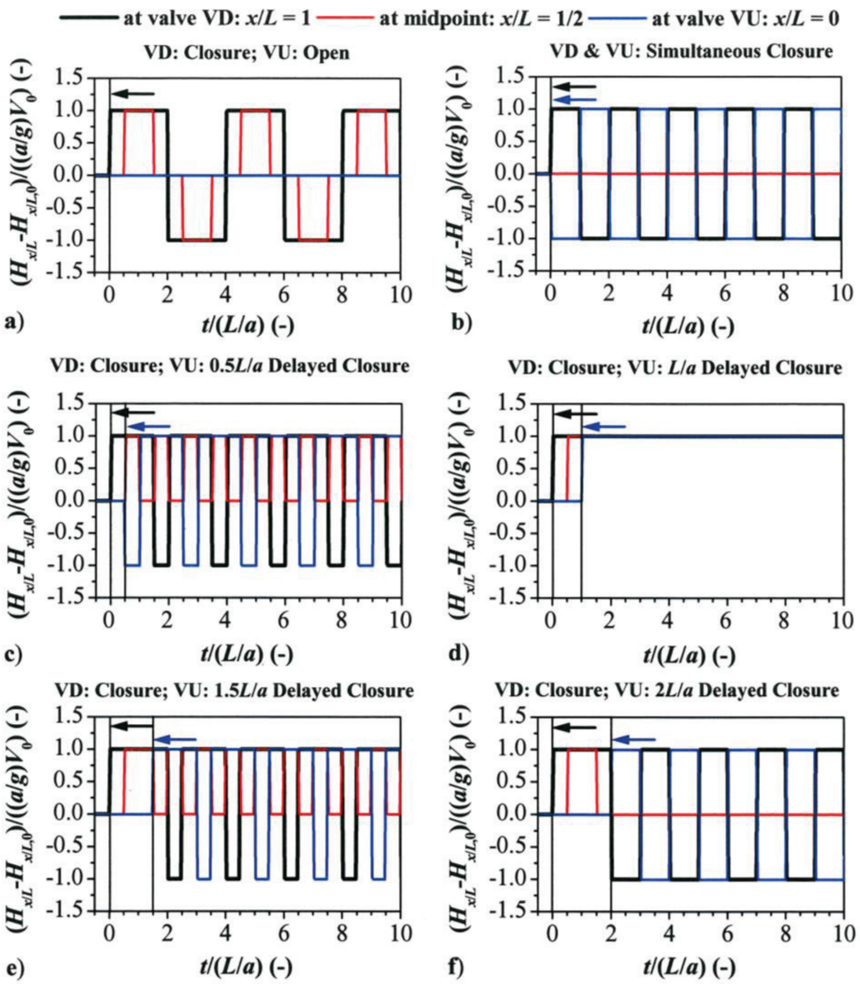

Figure 4: Dimensionless pressure head histories in the ideal reservoir-valve-pipe-valve system: Instantaneous closure of the end valves, first VD and then VU (time delay: $0 \leq t_{d,VU} \leq 2L/a$)

Figure 5 presents the pressure head response for the case of delayed closure of the upstream end valve VU with a time delay from $2L/a$ to $4L/a$. This period is actually the second round trip wave period in the conventional reservoir-pipe-valve system (Fig. 5a). As stated before, the flow situation induced by the second valve closure (VU) at time $2L/a$ after the first valve closure (VD; Figs. 4f and 5b) is similar to the situation of simultaneous valve closure (Fig. 4b). The delayed closure of the valve VU at the time of $2.5L/a$ and at $3.5L/a$ after VD closure shows a similar response (Figs. 5c and 5e). Pressure heads at valves VD and VU vary with a period of $2L/a$, respectively. Pressure head at the midpoint oscillates with a period of L/a, and it never exceeds the initial static head. The second valve closure (VU) at time $3L/a$ after the first valve closure (VD) is shown in Fig. 5d. The interference of two water hammer waves completely attenuates pressure oscillations in the pipeline. The pressure head drops below the initial static head exactly for the Joukowsky head (Eq. 2). In this case, the interferometer works as a pressure head suppressor.

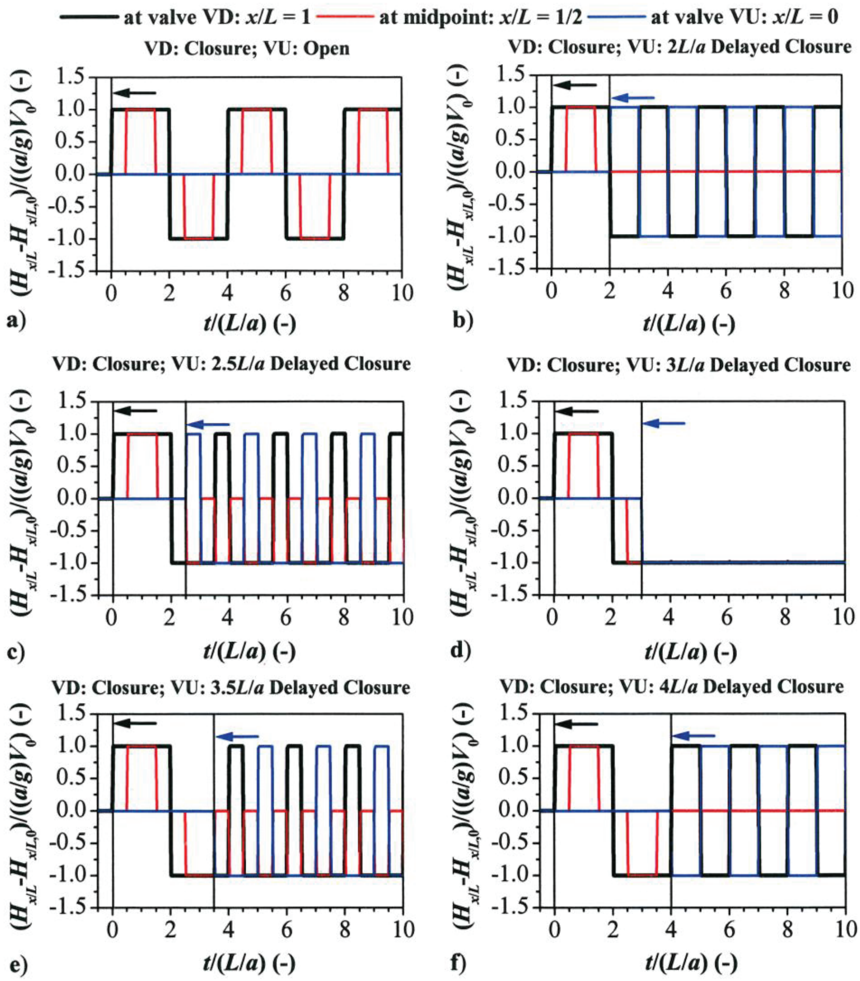

Figure 5: Dimensionless pressure head histories in the ideal reservoir-valve-pipe-valve system: Instantaneous closure of the end valves, first VD and then VU (time delay: $2 \leq t_{d,VU} \leq 4L/a$)

Investigation of the second valve closures within the time delay period of $2L/a < t_{d,VU} \leq 4L/a$ reveals exactly the same pressure response as produced in the range of $0 < t_{d,VU} \leq 2L/a$ but with the opposite pressure head sign. In essence, the wave physics of the water hammer response repeats with an integral theoretical period of $4L/a$ after the second valve closure (VU in our case). Within the frame of the integral theoretical period, there are a number of responses with periods of 2*L*/*a* and *L*/*a* and situations with constant pressure along the complete length of the pipeline. When one compares the conventional single-valve closure case with the two-valve closure one (Figs. 4 and 5), it is evident that the delayed closure of the second valve (VU in our case study) has a profound effect on the pressure head traces in the pipeline system.

4 CONCLUSIONS

This paper investigates the effects of multiple-valve closure (closure of upstream-end and downstream-end valves) on pressure head response. The system under consideration is a simple reservoir-valve-pipeline-valve system (two-valve system). The two valves can be closed either simultaneously, or one is shut with a time delay. This may produce large or low pressures heads depending on the valve control scenario. The system with two rapid closing far end valves generates two water hammer waves that superimpose (interfere) at some point along the pipeline. Superposition of waves can generate pressure heads of greater, lower or the same amplitude. Interference refers to the interaction of waves that are correlated or coherent with each other. The concept of an acoustic tube interferometer using controlled action of two valves is proposed. Because the two waves are water hammer waves, the device is called *water hammer interferometer*. The paper presents basic water hammer theory that is used for the detailed description of the interferometer. When one compares pressure response produced by the conventional single-valve closure with the one produced by the water hammer interferometer (two-valve closure), one finds that the time delay of closure of the second valve has a profound effect on the pressure head traces in the pipeline system.

References

[1] **E.B. Wylie, V.L. Streeter:** *Fluid Transients in Systems*, Prentice Hall, 1993

[2] **M.H. Chaudhry:** *Applied Hydraulic Transients,* Springer, 2014

[3] **A. Bergant, J.M.C. van't Westende, T. Koppel, J. Gale, Q. Hou, Z. Pandula, A.S. Tijsseling:** *Water hammer and column separation due to accidental simultaneous closure of control valves in a large scale two-phase flow experimental test rig*, Pressure Vessels and Piping Division Conference, ASME, Bellevue, Washington, USA, 2010

[4] **A. Bergant, U. Karadžić:** *Developments in valve-induced water-hammer experimentation in a small-scale pipeline apparatus*, 12th International Conference on Pressure Surges, BHR Group, Dublin, Ireland, 2015

[5] **Y. Liu, Z. Huang, C. Jiang:** *Characteristics of water hammer induced valve-valve system*, 2015 International Conference on Fluid Power and Mechatronics, IEEE, Harbin, China, 2015

[6] **S. Ikeo, T. Kobori:** *Water hammer caused by valve stroking in a pipe with two valves,* Buletin of JSME, JSME, Vol. 18, Iss. 124, p.p. 1151 – 1157, 1975

[7] **G.S. Chaddha:** *University Physics for Engineering and Science Students*, Alpha Science International Ltd, 2015

[8] *Interference (wave propagation)*, Wikipedia [world wide web], available at: http://en.wikipedia.org/wiki/Interference_(wave_propagation)/(19.12.2016)

[9] **Sir J.F.W. Herschel:** *On the absorbtion of light by coloured media, viewed in connection with undulatory theory,* The Philosophical Magazine, Vol. 3, Iss. 18, p.p. 401 – 412, 1833

[10] **G. Quincke:** *Ueber Interferenzapparate für Schallwellen,* Annalen der Physik und Chemie, Vol. 128, Iss. 6, p.p. 177 – 192, 1866

[11] **A. Bergant, A.S. Tijsseling, J.P. Vítkovský, D.I.C. Covas, A.R. Simpson, M.F. Lambert:** *Parameters affecting water-hammer wave attenuation, shape and timing. Part 1: Mathematical tools*, Journal of Hydraulic Research, IAHR, Vol. 46, Iss. 3, p.p. 373 – 381, 2008

[12] **A. Bergant, A.S. Tijsseling, J.P. Vítkovský, D.I.C. Covas, A.R. Simpson, M.F. Lambert:** *Parameters affecting water-hammer wave attenuation, shape and timing. Part 2: Case studies*, Journal of Hydraulic Research, IAHR, Vol. 46, Iss. 3, p.p. 382 – 391, 2008

Nomenclature

(Symbols)	(Symbol meaning)
a	water hammer wave speed
g	gravitational acceleration
H	piezometric (pressure) head
L	length
p	pressure
V	flow velocity
t	time
t_d	time delay
x	distance
ΔH	pressure head change
Δp	pressure change
ΔV	flow velocity change
ρ	mass density

(Subscripts)	(Subscripts meaning)
mp	midpoint
VD	downstream end valve
VU	upstream end valve
0	initial conditions

(Superscripts)	(Superscripts meaning)

(Abbreviations)	(Abbreviations meaning)
VD	downstream end valve
VU	upstream end valve

Acknowledgments

The author wishes to thank Slovenian Research Agency (ARRS) for the support of this research conducted through the project L2-5491 (ARRS).

Journal of Energy Technology

JET Volume 9 (2016) p.p. 21-34
Issue 4, December 2016
Type of article 1.01
www.fe.um.si/en/jet.html

DEVICE FOR THE MANUFACTURING OF OVENS BY RESISTANCE SEAM WELDING

NAPRAVA ZA IZDELOVANJE PEČIC Z UPOROVNIM KOLUTNIM VARJENJEM

Zdravko Praunseis[ℜ], Seudin Softić [1]

Keywords: eresistance welding, seam welding, oven line FS16, automation line

Abstract

In the industries that simultaneously require large productivity and high reliability, it is necessary to invest much time in different studies and to choose the right equipment for the desired product. While we were designing an automated line for the production of FS16 ovens, we encountered a variety of challenges, because we used equipment that is mostly unknown in our environment. In this article, the basic device for resistance seam welding is described. Various forms of the welds are also described.

The device itself will have a huge role in the operation of the line; therefore, it was very precisely constructed and designed.

Povzetek

V industrijah, kjer se zahteva velika produktivnost in hkrati velika zanesljivost izdelkov, je treba vložiti veliko časa v razne študije in izbrati ustrezno opremo za konstrukcijo ciljnega izdelka. Pri projektiranju avtomatske linije za proizvodnjo pečice FS16 smo se srečali z najrazličnejšimi izzivi, saj smo uporabili opremo, ki je v našem okolju še neznana. V članku je opisana naprava za uporovno kolutno varjenje in različne oblike zvarov.

Naprava ima pomembno vlogo pri delovanju delovne linije, zato je natančno oblikovana in konstruirana.

ℜ Corresponding author: Zdravko Praunseis, Faculty of Energy Technology, University of Maribor, Tel.: +386 70 286 719, Mailing address: Hočevarjev trg 1, Krško, Slovenia, E-mail address: zdravko.praunseis@um.si

[1] Gorenje d.d., Partizanska 12, Velenje, Slovenia

1 INTRODUCTION

Therefore, it is necessary to make hypotheses before we start designing, and attempt to confirm or reject them. The purpose of this master's thesis is also to generally demonstrate the welding of steel constructions and the factors that are important for quality welded joint. The theoretical background knowledge is then demonstrated on the seam welding device itself. For the quality design of the device, a great deal of various knowledge is necessary. The main factors to design and realise welded joints are: characteristics of the steel, sort of loads, different varieties of welding, sort of adding materials, etc. Appropriate choice of equipment and welding procedure is a major factor. Regular maintenance is necessary to ensure a long functioning of the device without problems. The biggest focus is on cooling of the electrodes, the control unit, and the transformer. Because of the very large current that flows through those elements, the thermal burdens are enormous. They must be surrounded with a cooling liquid. Care must be taken not to produce any condensate in those elements.

2 EXPERIMENT AND RESULTS

Welding is implemented on two joints, where the plates of U-circumference and ceiling overlap by a few millimetres, *[6]*.

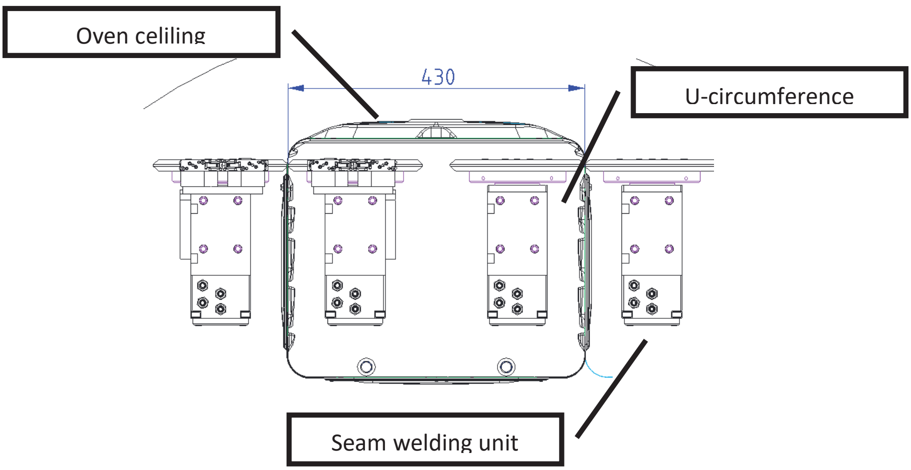

Figure 1: *Welding sketch*

Ceilings are taken from a specially modified transporter with a robot arm with a pneumatic gripper, and they are additionally positioned on a special unit in X,Y directions.

Ceilings are then delivered to a rotatable unit, where they are positioned on lateral glands and vacuum clamped. The U-circumference is loaded with a line manipulator (two-dimensional manipulator with several sequential grippers). The robot transfers the U-circumferences with a pneumatic gripper from a U-bending station to a line manipulator entry place, *[4]*.

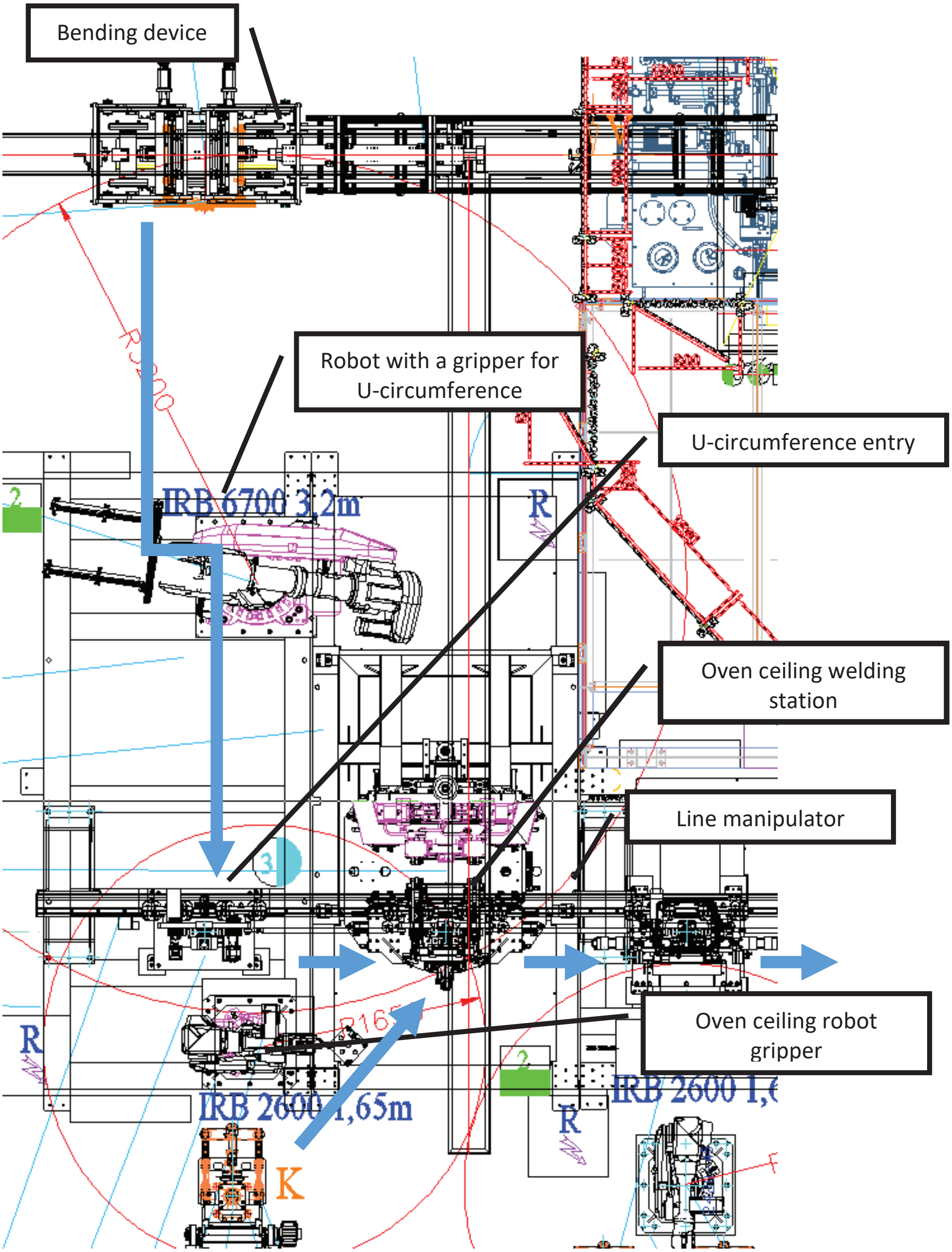

Figure 2: *Station's ground plan*

The line consists of four main connecting segments:

- U-circumference formation,
- composing and welding of the oven,
- manufacturing the oven's back end,
- transport system.

There is an unwinding station with a lifting unit for a sheet reel at the beginning of the line. After the straightening and cutting station is the station for storing cut sheets, which ensures smooth line functioning during the sheet reel exchanges.

After that, there is a station for the lubrication of cut sheets and a serving unit that transfers the sheets further in the presses, which contains hole-cutting tools, and after that on a conveyor. The U-bending station is at the end.

The robot is transmitting the U-circumference with a gripper on a composition and welding part of the line. The main feature of that part of the line is a line manipulator with 14 grippers, which are transferring ovens from one station to the other at the same time. In this part of the line, there are stations for welding and shaping different oven assembly parts. At the end of that part of the line, the carriers for enamelling are being welded. At the very end of the welding line, there is a unit for the automatic assembly and welding of the oven and front end, where the robot with a pneumatic gripper is transferring the front ends from a line storage container. A set of stations for manufacturing of the back ends serves for production of many variants of cut back ends and shapes. Back ends are delivered from line storage transporters and a robot with a pneumatic gripper on to a welding station. Custom-designed welding units are spot welding the housing of the oven with front ends, *[4].*

The station for ceiling welding has the following key features:

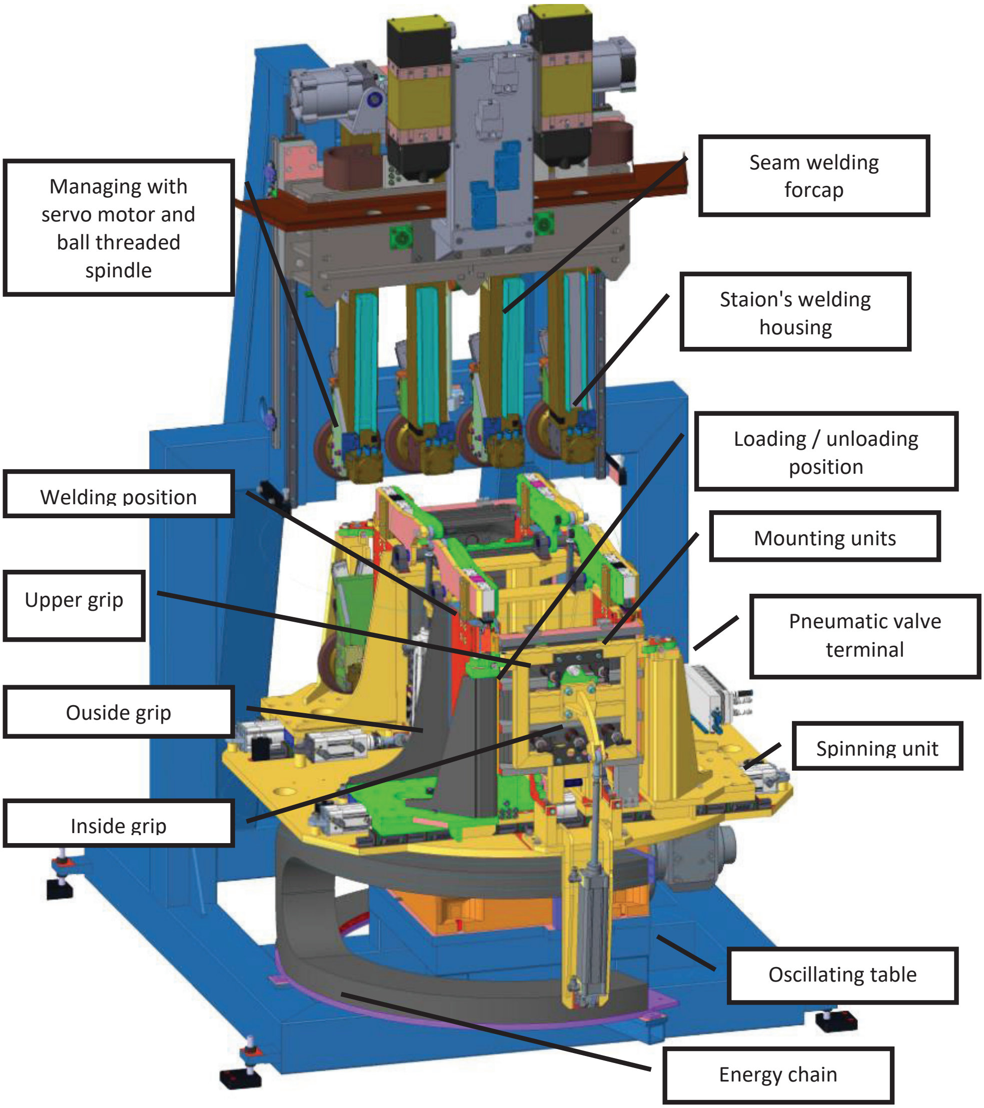

Figure 3: *Final station for oven ceiling welding*

Because of short deadlines, designing this kind of station is a process in which it is necessary to accept the decisions that affects the reliability, power consumption, welding quality, dimensions, appearance and price. All these criteria must be optimally coordinated for the success of a project. We can highlight two arguments among all the others.

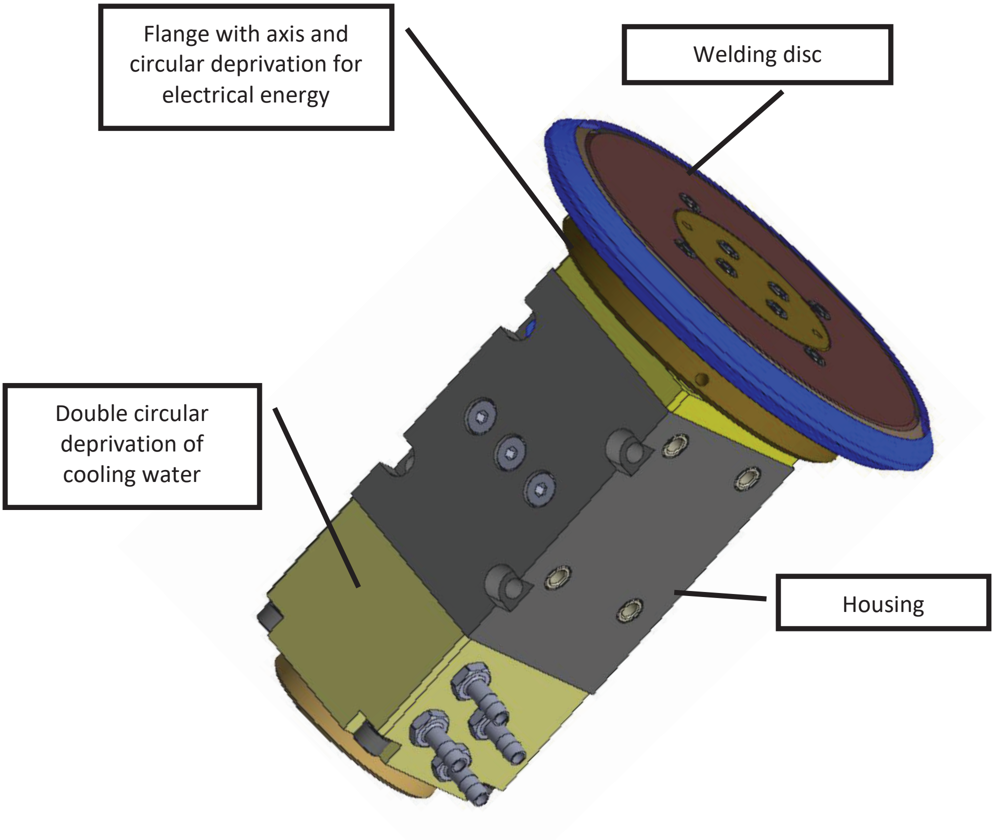

Figure 4: *Seam welding unit*

The transition of electrical energy from the frame to rotary axis is executed with a special space that is sealed and contains a conducting material. Previously, mercury was used, but it is currently forbidden because of environmental standards. Because of welding and the enormous amount of conducting electrical energy, conductor heating occurs. Extraction of that heat is ensured with the supply of cooling water. Two units for seam welding are installed on the seam welding forceps, *[6].*

Forceps for seam welding are vital at that station, among the correct mounting of the sheets. Actuating valves ensure the force needed for welding. The force is set automatically through the welding control unit according to the welding parameters and current welding conditions. In Figure 5, the principal forceps elements are shown.

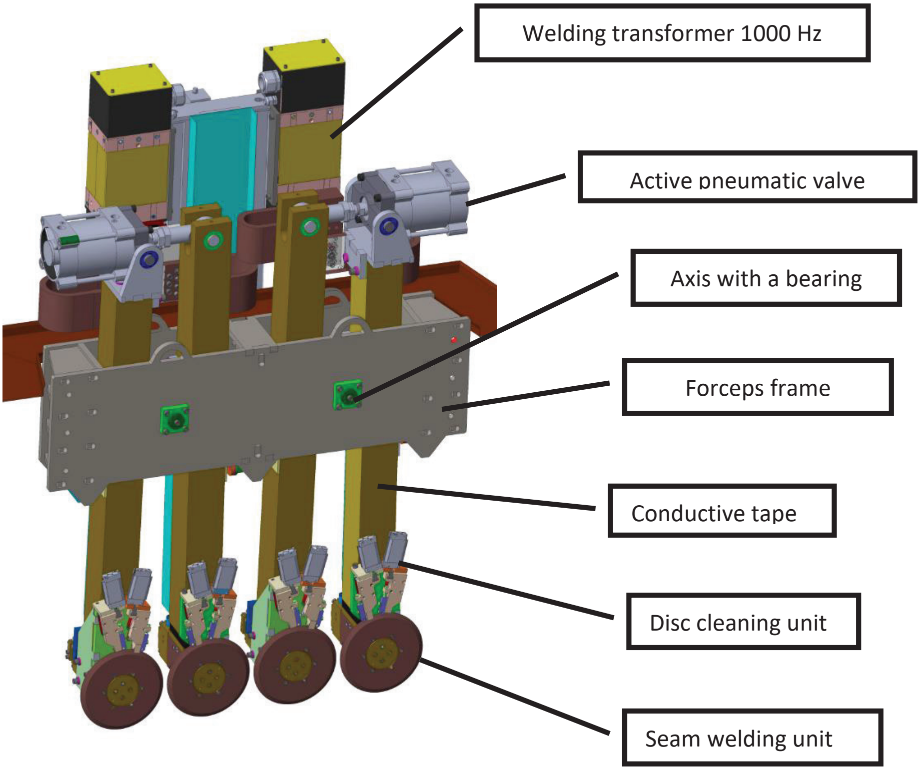

Figure 5: *Seam welding forceps*

Through tests that were made at different line and welding components, it was concluded that we need a principle of two seam welders for each welded joint to ensure quality welding. The previous version of the station (2008) contained a seam on a straight electrode. The principle worked, but it no longer ensures sufficient quality for new demands; the sheet on the inner side was not adequately merged to the ceiling; therefore, an edge was visible. Implementing seam forceps improved the quality of the final product.

The cooling is determined according to the type of weld, number of welds per minute, the size of the current, and the cross-section of secondary conductors. Direct cooling of the tip of the electrode would be ideal, as shown on Figure 6. That way, a direct extraction of the heat is ensured. The life span is extended, and the welding lenses and joints are of higher quality, *[4].*

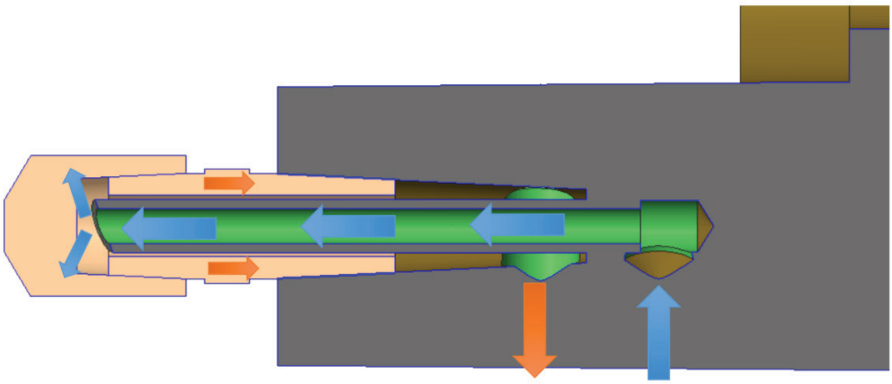

__Figure 6:__ Supply and drain of the cooling water for electrodes

Legend:

 Cooling water supply (cooled water)

 Cooling water drain (heated water)

Without the cooling of the electrodes, they would eventually reach material-melting temperature. As they are heat strengthened materials, all good mechanical characteristics that they got during the heat treatment would be lost. If the electrodes are extremely heated, so-called bonding of material on the electrode occurs, and working geometry is corrupted, which is followed by large amounts of melted metal spraying at the next weld. Much improper cooling would take place.

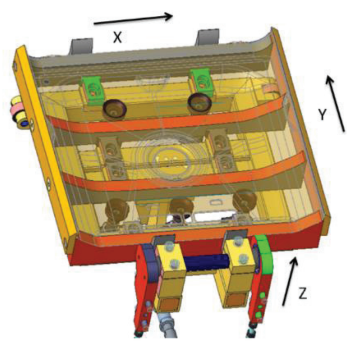

__Figure 7:__ Ceiling placement in X,Y directions

Up and down, the ceiling sheets are placed separately in Z directions (Figure 8) so as to prevent dimension inaccuracy.

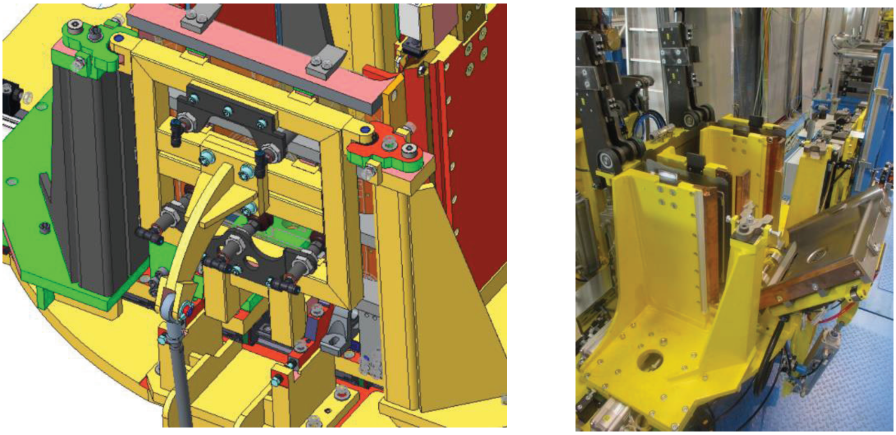

Figure 8: *Ceiling placement in Z directions*

The U-circumference and the oven ceiling must be correctly positioned in a final stage of disposal. When they are in position and mounted, the device is ready for the seam welding.

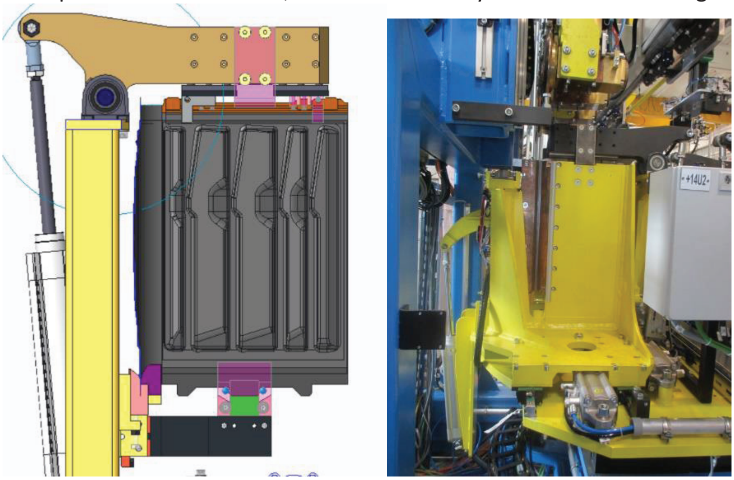

Figure 9: *U-circumference and the oven ceiling are ready for seam welding*

At the starting point the seams are in the top position and spaced from each other. The down move is executed by a servo motor, *[4].*

The first position is 10 mm above the oven, where a weld joint is made. We made a joint to prevent a deviation of the U-circumference and the ceiling of the oven.

Figure 10: *The position of weld joint that prevents U-circumference and ceiling deviation*

When we are done with a weld joint, the welding disk performs a down move to a position 2 mm above the bottom edge of the oven. It is very important that we move the disks as close to the edge of the oven as we can, so that we prevent the deviation of the U-circumference and the ceiling of the oven.

Figure 11: *Bottom position of seam weld*

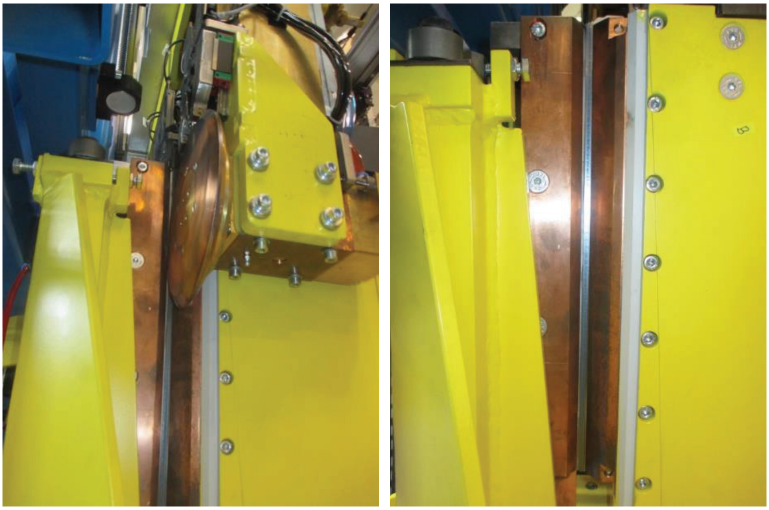

Figure 12: *Upper position of seam weld*

Figure 13: *An example for welded U-circumference and front end.*

The BOS 6000 program is specially adapted to manage all BOSCH controllers. The program allows us to adapt the blocks and welding programs. In each block or program, we can set the required parameters, such as time of prepressing, pressing, welding, cooling, etc. Among all time parameters, we can also set the type of welding (point, seam) and the pressure of the seams to the welders. Those were the most frequent parameters used in this project. Of course, many other parameters and functions can also be set.

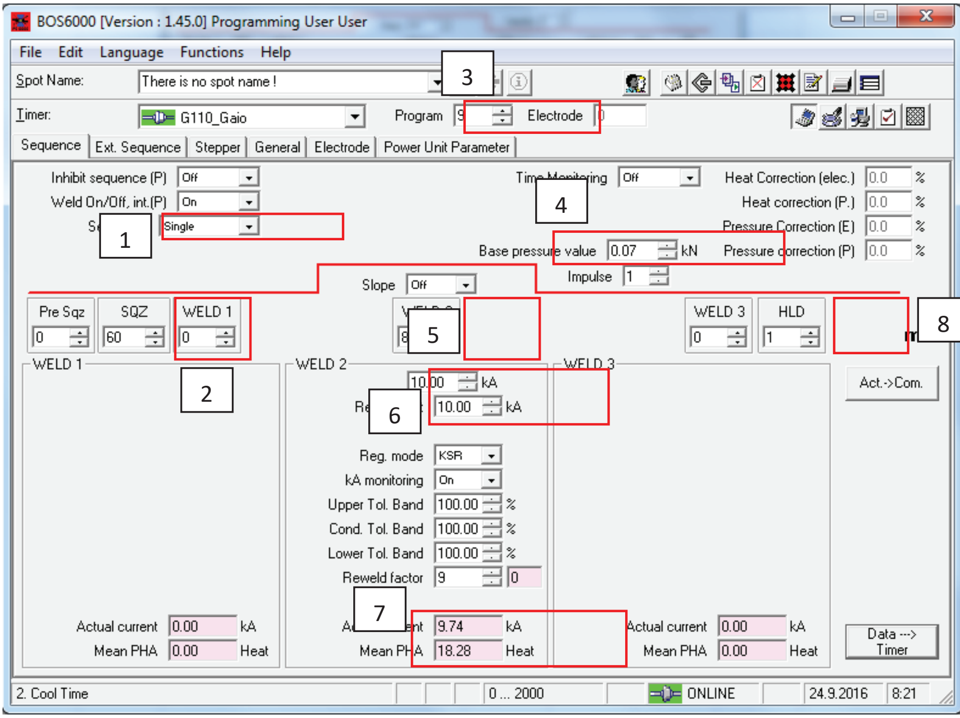

Figure 14: *Spot-welding parameters*

This station is highly productive, as are all other stations, which is why they are all crucial for the production of the line. In case of an error, the mistake must be easily and quickly repaired.
A permanent dynamic test is ensured for most of the elements of the station. The machines are designed so as to predict the places of installations and the easy ways to replace spare parts, *[4-6]*.

Example of maintenance:

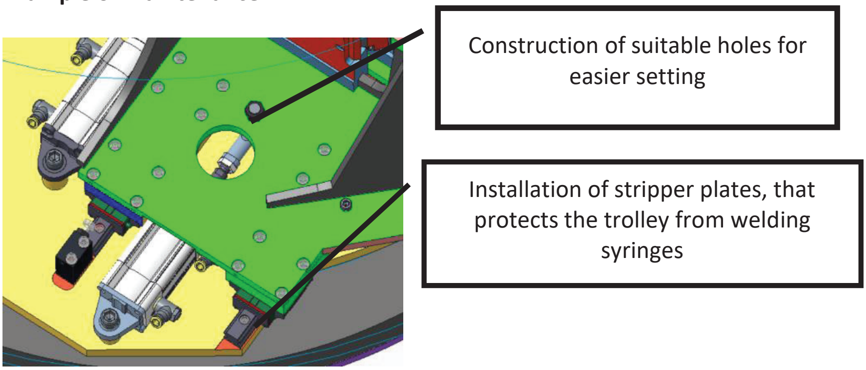

Figure 15: *Linear feed composition*

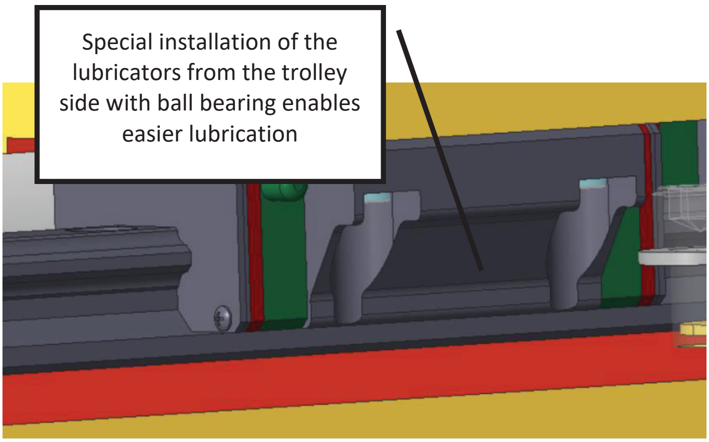

Figure 16: *Mounting of side lubricating nipple on to a trolley*

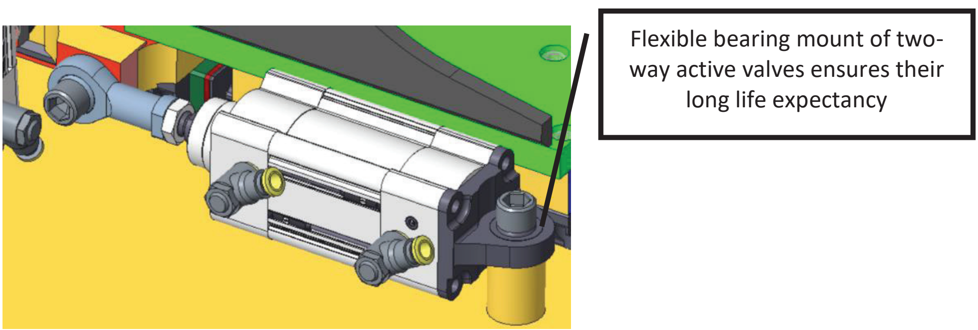

Figure 17: *Mounting of active pneumatic valve*

3 CONCLUSION

Designing or constructing seam-welding devices have been developing dramatically lately. The designers have a huge advantage in the possibility to work in sophisticated and advanced software, so they can imagine how to improve the device and make it more efficient. In this master's thesis, I concentrated on the process of welding, which are modified and improved through time. We learn about new ways of welding metal and other materials; accordingly, we must construct a welding device. For the purposes of production in the company Gorenje Mora in the Czech Republic, we constructed a device and placed on an automated line, so as to exclude the human factor and reduce the chance of an error; the merging also became much faster. The device needs about 10 seconds to complete a weld, while a person would spend much more time for the same work. We encountered many mechanical and software problems at the start up. To have a quality weld, it is crucial to know the material that is being worked on. We have learned that the cooling of the heating components is also very important. Two ways were available: air or water cooling. Based on good experiences, we decided to cool the components with water. The investments in this project are enormous, but the company's vision is to automate the production as much as possible. Any parameter changes can be implemented through a control panel on a control desk, which is placed near a device. The seam welding discs are being used up over time, therefore the parameters as disc pressure or secondary current on the transformer must also be adjusted.

References

[1] **S. Pehan**: *Metodika konstruiranja: univerzitetni učbenik – Maribor*, Fakulteta za strojništvo, 2005

[2] **B. Kraut**: *Krautov strojniški priročnik,* 14. Slovenska izdaja / izdajo pripravila Jože Puhar, Jože Stropnik. Ljubljana: Littera picta, 2003

[3] **Z. Praunseis**: *Energetski inženiring, Zapiski predavanj*, Fakulteta za energetiko, 2015

[4] **S. Softić**: *Welding machine for cavity FS16 with resistance spot welding method, Master Thesys in progress*, Faculty of energy technology, 2016

[5] **B. Hudej**: *Koncipiranje in snovanje postaje za varjenje stropa pečice: diplomsko delo – Maribor*, Fakulteta za strojništvo, 2016

[6] **Z. Praunseis**: *Točkovno uporovno varjenje nerjavnega bobna pralnega stroja, tehniško poročilo o raziskavi*, Fakulteta za strojništvo, 2003

Journal of Energy Technology

JET Volume 9 (2016) p.p. 35-42
Issue 4, December 2016
Type of article 1.01
www.fe.um.si/en/jet.html

THE APPLICATION OF FUZZY LINEAR PROGRAMMING METHODS IN ENERGY PLANNING

UPORABA METOD MEHKEGA LINEARNEGA PROGRAMIRANJA V ENERGETSKEM NAČRTOVANJU

Maja Repnik[ℜ]

Keywords: fuzzy linear programming, fuzzy constraints, fuzzy numbers, energy planning, R package FuzzyLP.

Abstract

Very frequently some of the parameters of certain optimization problems solvable by linear programming cannot be precisely determined. In this case, fuzzy linear programming techniques can be used. In the relevant literature, there are many real-world problems solved by fuzzy linear programming methods, but they are scarce in the field of energy technology. The main reason for that might be the lack of effective software for solving fuzzy linear programming problems. In 2015, researchers developed the R package FuzzyLP, software for public use, which solves fuzzy linear programming problems directly. The potential that real world problems from different fields, including energy planning, can be solved using fuzzy linear programming methods by researchers who do not necessarily have knowledge of fuzzy linear programming can be seen. . To illustrate its application, we solve two small examples using the fuzzy linear programming methods and compare them with a case in which all parameters are precisely defined.

ℜ Corresponding author: Maja Repnik, University of Maribor, Faculty of Energy Technology, Tel.: +386 7 620 2219, Mailing address: Hočevarjev trg 1, 8270 Krško, Slovenia, E-mail address: maja.repnik@um.si

Povzetek

V optimizacijskih problemih, ki jih rešujemo z uporabo linearnega programiranja, se pogosto zgodi, da nekaterih koeficientov ne moremo natančno določiti. V tem primeru lahko uporabimo mehko linearno programiranje. V literaturi najdemo veliko problemov iz resničnega življenja, ki so rešeni z uporabo mehkega linearnega programiranja, a na področju energetike so le redki. Glavni razlog za to je najbrž pomanjkanje učinkovite programske opreme. Raziskovalci so leta 2015 razvili R paket FuzzyLP, ki je program, dostopen javnosti in ki direktno rešuje probleme mehkega linearnega programiranja. S tem je področje dobilo potencial, da bi raziskovalci z različnih področij, vključno z energetskim načrtovanjem, ki nimajo nujno znanja iz mehkega linearnega programiranja, začeli uporabljati mehko linearno programiranje za reševanje problemov. Uporabo smo ponazorili z dvema manjšima zgledoma, ki smo ju rešili s pomočjo treh metod za reševanje problemov mehkega linearnega programiranja. Za primerjavo smo najprej rešili primer linearnega programa, kjer so vsi koeficienti natančno določeni.

1 INTRODUCTION

Linear programming (LP) is one of the most frequently used techniques in operations research. In real world problems, some parameters of LP frequently cannot be precisely determined. We can model imprecise parameters using fuzzy sets, which were introduced by Lotfi A. Zadeh in *[8].* Zimmermann then proposed the formulation of fuzzy linear programming (FLP) problems in *[9]*. Since then, researchers have developed a relatively large number of different methods to solve FLP problems. A general model of an LP problem can be written as

$$\begin{aligned} \text{maximize} \quad & cx \\ \text{subject to} \quad & Ax \leq b \\ & x \geq 0. \end{aligned}$$

If some of the coefficients (c, A, b) cannot be precisely defined we can treat them as fuzzy numbers (notation for fuzzy number a is $\tilde{a}$) and call this LP problem the FLP problem. Based on the place where fuzzy numbers appear, we can divide FLP problems into four main categories:

- FLP with fuzzy resources ($\tilde{b}$);
- FLP with fuzzy coefficients in objective function ($\tilde{c}$);
- FLP with fuzzy technological coefficients ($\tilde{a}_{ij}$);
- FLP with fuzzy variables ($\tilde{x}$).

By combining these four categories, we obtain many different types of FLP problems, each of which is solvable with a different method. Authors use different indices to compare fuzzy numbers in their methods, accompanied by different shapes of fuzzy numbers, different computational methods, etc. In light of all these issues, it is easy to understand that there are a plethora of different methods to solve FLP problems. Around 50 methods have been analysed, and a basis for a taxonomy of FLP methods has been published in *[3].*

2 ENERGY MODELS USING FLP

Although researchers have used FLP methods to solve problems in various fields, there are only a few examples of this in the field of energy technology (e.g. *[4], [7]*). In *[5]*, Sadeghi and Hosseini outlined that FLP is an effective approach that has not been attended extensively in energy planning field up to now. They stated the main obstacles in confronting the FLP approach, including unfamiliarity, a lack of favour in academic circles, and a lack of effective and comprehensive software. They wanted to overcome the lack of software with a fuzzy version of GAMS, a popular algebraic modelling language for crisp mathematical programming. However, the idea was only briefly outlined, and no further development has been done.

3 SOFTWARE FOR SOLVING FLP PROBLEMS

Most researchers illustrate new methods on small examples that can be solved without any software. Other researchers who want to solve real-world problems with the FLP method, firstly defuzzify the FLP problem, by converting it to a crisp optimization problem, which can be easily solved with existing software. They convert FLP to an LP, parametric LP, multi-objective linear programming problem, non-linear programming problem or semi-infinite LP.

In 2015, researchers at the University of Granada presented an open-source R package named FuzzyLP, *[2]*, to deal with fuzzy constraints, fuzzy costs and fuzzy coefficients in linear programming. R package FuzzyLP is the only software written in modern language developed for public use that solves FLP problems directly. The package can be freely downloaded, employed, and extended by any R user. The authors hope their work will contribute to further software developments to make fuzzy mathematical programming models available for researchers and practitioners from other areas, spreading this methodology beyond the fuzzy community.

4 EXAMPLES

Let us demonstrate the use of some FLP methods on small examples. In Example 1, borrowed from *[6],* we solve a conventional LP problem, and the solution is compared with solutions of Example 2 and Example 3, which are FLP problems.

Example 1

Electricity is produced at a small thermal plant with the use of system turbine/generator. The turbine is rotating with the help of $3.2\ kg/s$ water steam. The owner can sell

- electricity at 0.03 EUR per kWh;
- High-pressure technical steam (x_1) at price 1.65 EUR per tonne;
- Low-pressure steam for central heating (x_2) at 1.10 EUR per tonne.

Customers are interested in unlimited quantities of electrical power, but for the amount of steam they have the following limitation:

$$4x_1 + 3x_2 \leq 9.6.$$

Generator power (in kW) depends on the flux of steam (in kg/s) through the parts of the turbine (I, II and III):

$$P_I = 48\, m_I \quad P_{II} = 56\, m_{II} \quad P_{III} = 80\, m_{III}\ .$$

To prevent the low-pressure part of the turbine from being overheated there must be a flux of steam through part III of at least 0.6 kg/s. To prevent unequal overload of a turbine shaft for $x_1 = 0$ kg/s it is permitted $x_2 = 1.8$ kg/s, but by increasing the use of steam x_1 for every kg/s decreases the use of steam x_2 for 0.25 kg/s. Set the optimal production.

First, we need to find an objective function that evaluates the income of a thermal plant. Faced with the need to make some calculations, which are basic in linear programming, to construct objective functions, we obtain the results that income from sold electricity to be $17.66 - 4.08x_1 - 2.40x_2$, income from high pressure steam to be $1.65 \cdot 3.6\, x_1$ and income from low pressure steam to be $1.10 \cdot 3.6\, x_2$. This implies that we have to maximize function

$$z = 17.66 - 4.08x_1 - 2.40x_2 + 1.65 \cdot 3.6\, x_1 + 1.10 \cdot 3.6\, x_2,$$

when variables x_1 and x_2 satisfy the described conditions. To set the optimal production we need to solve the following linear programming problem:

$$\max z = 1.86x_1 + 1.56\, x_2$$

subject to

$$\begin{aligned} x_1 + x_2 &\le 2.6 \\ x_1 + 4x_2 &\le 7.2 \\ 4x_1 + 3x_2 &\le 9.6 \\ x_1, x_2 &\ge 0. \end{aligned} \qquad (4.1)$$

The solution of (4.1) can easily be obtained, and it is $x_1 = 1.8$, $x_2 = 0.8$ and $z_{max} = 4.6$. That implies that for optimal production they should sell 1.8 kg/s high pressure technical steam and 0.8 kg/s low pressure steam for central heating. The rest of the steam would be used for electricity production. The income would be €22.26 per hour.

Example 2

Suppose we have the same thermal plant as in Example 1, but the price of high-pressure technical steam (x_1) and the price of low pressure steam for central heating (x_2) cannot be predicted in advance. They can predict that the price for high pressure technical steam (x_1) would be around €1.65 per tonne, in worst case can be only €1.30 per tonne and the price can also rise to €1.70 per tonne. This suggests that we can treat the price of high pressure technical steam as a fuzzy number. There are many different shapes of fuzzy numbers described in the literature (linear, exponential, Gaussian, etc.) but the most frequently used shape of the membership function is linear, which defines triangular and trapezoidal fuzzy numbers. The price for high pressure technical steam as a triangular fuzzy number ($\tilde{c}_1$) can be presented with the membership function in Figure 1

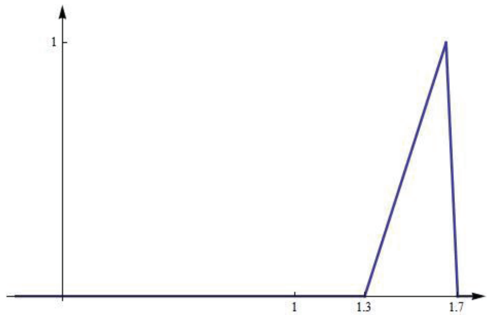

Figure 1: ***Membership function of fuzzy number*** $\tilde{c}_1$

and can be written as $\tilde{c}_1 = (1.3, 1.65, 1.7)$. Moreover, the price for low pressure steam for central heating can be treated as a triangular fuzzy number, for example $\tilde{c}_2 = (0.95, 1.10, 1.14)$. We need to maximize the function:

$$z = 17.66 - 4.08x_1 - 2.40x_2 + (1.3, 1.65, 1.7) \cdot 3.6\, x_1 + (0.95, 1.10, 1.14) \cdot 3.6\, x_2$$

equals to

$$z = 17.66 + (0.6, 1.86, 2.04)x_1 + (1.02, 1.56, 1.7)x_2.$$

Now, the problem (4.1) becomes an FLP problem with fuzzy parameters in the objective function:

$$\max z = (0.6, 1.86, 2.04)x_1 + (1.02, 1.56, 1.7)x_2$$

subject to

$$\begin{aligned} x_1 + x_2 &\leq 2.6 \\ x_1 + 4x_2 &\leq 7.2 \\ 4x_1 + 3x_2 &\leq 9.6 \\ x_1, x_2 &\geq 0. \end{aligned} \tag{4.2}$$

There are many different methods described in the literature that can be used to solve problem (4.2). In the FuzzyLP package, we can choose from among five different functions that solve FLP problem with fuzzy parameters in objective function. Here Delgado's approach, *[1]*, is used, which in package FuzzyLP with function FOLP.multiObj is implemented. We use the following code:

```
obj <- c(TrapezoidalFuzzyNumber(0.6,1.86,1.86,2.04),
TrapezoidalFuzzyNumber(1.02,1.56,1.56,1.7))
A<-matrix(c(1, 1, 4, 1, 4, 3), nrow = 3)
dir <- c("<=", "<=","<=")
b <- c(2.6, 7.2, 9.6)
max <- TRUE
sal<-FOLP.multiObj(obj, A, dir, b, maximum = max, min=0, max=1, step=0.1)
sal
sal[,"objective"]
```

and the solution:

```
     alpha x1       x2       objective
 [1,] 0     1.8      0.8       ?
```

```
 [2,] 0.1   1.8      0.8      ?
 [3,] 0.2   1.8      0.8      ?
 [4,] 0.3   1.8      0.8      ?
 [5,] 0.4   1.8      0.8      ?
 [6,] 0.5   1.8      0.8      ?
 [7,] 0.6   1.8      0.8      ?
 [8,] 0.7   1.8      0.8      ?
 [9,] 0.8   1.8      0.8      ?
[10,] 0.9   1.066667 1.533333 ?
[11,] 1     1.066667 1.533333 ?
 [[1]]
Trapezoidal fuzzy number with:
   support=[1.896,5.032],
      core=[4.596,4.596].
```
... output omitted for list elements 2 to 10.
```
[[11]]
Trapezoidal fuzzy number with:
   support=[2.204,4.78267],
      core=[4.376,4.376].
```

To understand the solution, we need to explain what alpha $\boldsymbol{\alpha}$ represents. If we denote $\boldsymbol{\mu}(\boldsymbol{C}) = \inf_{j} \boldsymbol{\mu}_{\tilde{c}_j}(\boldsymbol{x})$, where $\boldsymbol{\mu}_{\tilde{c}_j}(\boldsymbol{x})$ are membership functions off fuzzy parameters $\tilde{\boldsymbol{c}}_j$ for all $\boldsymbol{j}$ in objective function of FLP (4.2), then

$$\boldsymbol{\mu}(\boldsymbol{C}) \geq \mathbf{1} - \boldsymbol{\alpha}$$

is one of the conditions in defuzzified FLP (4.2). The lower value of $\boldsymbol{\alpha}$ leads to a higher expectation that the value of $\tilde{\boldsymbol{c}}_j$ will be very close to its core. From the solution report, we can see that for $\boldsymbol{\alpha} \leq \mathbf{0.8}$ the solution of FLP is the same as in a crisp case (Example 1). In contrast, the optimal solution changes for $\boldsymbol{\alpha} \geq \mathbf{0.9}$. Optimal value (objective) is a fuzzy number, which is here presented by its core and support. We observe that optimal value for $\boldsymbol{\alpha} \geq \mathbf{0.9}$ has broader support and a smaller core than optimal value for $\boldsymbol{\alpha} \leq \mathbf{0.8}$. This suggests that a very pessimistic decision maker should decide to implement the solution that we obtained for $\boldsymbol{\alpha} \geq \mathbf{0.9}$. The core of income will be a bit lower than for solution $\boldsymbol{x_1} = \mathbf{1.8}$, $\boldsymbol{x_2} = \mathbf{0.8}$, but the risk will also be lower.

Example 3

Now let us assume that in the thermal plant from Example 1 the condition of the flux of steam through Part III can be violated. It should be at least $0.6\ kg/s$, but in favour of better income they permit violation up to $0.1\ kg/s$. They want low violation of constraint and at the same time high profit. So we need to find compromise. Crisp value $b_1 = 2.6$ becomes fuzzy number $\tilde{b}_1$ with linear membership function in Figure 2.

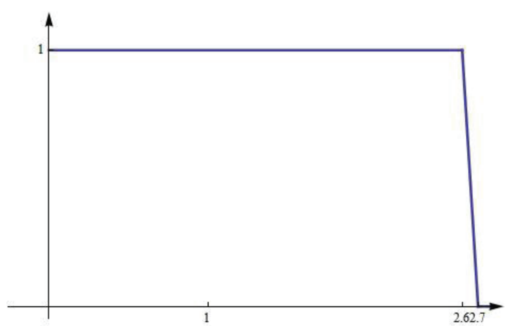

Figure 2: *Membership function of fuzzy number* $\tilde{\boldsymbol{b}}_1$

To solve this problem, we need to solve the following FLP problem with fuzzy resources:

$$\max z = 1.86x_1 + 1.56\, x_2$$

subject to

$$\begin{aligned} x_1 + x_2 &\leq 2.6 + (1-\beta)\cdot 0.1 \\ x_1 + 4x_2 &\leq 7.2 \\ 4x_1 + 3x_2 &\leq 9.6 \\ x_1, x_2 &\geq 0. \end{aligned} \tag{4.3}$$

Researchers have proposed many different methods for solving problem (4.3). Six of them are implemented in the FuzzyLP package. First, let us use Verdegay's approach that yields parametric solution. The code

```
obj <- c(1.86, 1.56)
A<-matrix(c(1, 1, 4, 1, 4, 3), nrow = 3)
dir <- c("<=", "<=","<=")
b <- c(2.6, 7.2, 9.6)
t <- c(0.1, 0, 0)
max <- TRUE
FCLP.sampledBeta(obj, A, dir, b, t, min = 0, max = 1, step = 0.2)
```

yields solution

```
    beta  x1   x2     objective
[1,]  0.0 1.50 1.20   4.6620
[2,]  0.2 1.56 1.12   4.6488
[3,]  0.4 1.62 1.04   4.6356
[4,]  0.6 1.68 0.96   4.6224
[5,]  0.8 1.74 0.88   4.6092
[6,]  1.0 1.80 0.80   4.5960
```

For each β that sets violation, we calculated the optimal solution and optimal value (objective). Now, the decision maker can decide what violation to permit (smaller β higher violation and better optimal value).

If the decision maker cannot decide on one solution, Zimmerman and Werners proposed compromise. This can be calculated with the code

```
FCLP.fuzzyUndefinedObjective(obj, A, dir, b, t, maximum=max, verbose = TRUE)
```

which yields solution

```
     beta  x1  x2  objective
[1,]  0.5 1.65  1    4.629
```

The best compromise between violation and optimal value is then achieved for $\beta = 0.5$, so the flux of steam through the part III would be at least $0.55 kg/s$ and then the income of the plant would be €22.29 per hour.

5 CONCLUSION

In the field of energy technology, there only a few problems are solved by fuzzy linear programming methods. But one of the main reasons for that, lack of effective software, can now be eliminated. With the use of R packet FuzzyLP, problems of bigger dimensions can also be solved, and the user does not need to have knowledge of fuzzy linear programming. In this paper, we demonstrated the application of fuzzy linear programming methods in an optimization problem of a small thermal plant to encourage other researchers and practitioners to use fuzzy linear programming methods to solve the real world problems that they are dealing with.

References

[1] **M. Delgado, J. Verdegay, and M. Vila***: Imprecise costs in mathematical programming Problems,* Control and Cybernetics, 16(2):113–121, 1987

[2] **C. A. Rabelo***: FuzzyLP: Fuzzy Linear Programming*, R package version 0.1-3, 2015

[3] **M. Repnik and D. Bokal***: A basis for taxonomy of fuzzy linear programming Methods,* In 13th International Symposium on Operational Research in Slovenia, Bled, Slovenia, September 23-25, 2015. ZADNIK STIRN, Lidija (ur.), et al. SOR '15 proceedings, pages 188–192. Ljubljana: Slovenian Society Informatika, Section for Operational Research, 2015

[4] **M. Sadeghi and H. M. Hosseini***: Energy supply planning in Iran by using fuzzy linear programming approach (regarding uncertainties of investment costs),* Energy policy, 34(9):993–1003, 2006

[5] **M. Sadeghi and H. M. Hosseini***: Evaluation of fuzzy linear programming application in energy models*, International Journal of Energy Optimization and Engineering (IJEOE), 2(1):50–59, 2013

[6] **W. F. Stoecker:** *Design of thermal systems*, New York: McGraw Hill Book Company, 1980

[7] **K. Tomsovic:** *A fuzzy linear programming approach to the reactive power/voltage control problem,* Power Systems, IEEE Transactions on, 7(1):287–293, 1992

[8] **L. A. Zadeh:** *Fuzzy sets*, Information and control, 8(3):338–353, 1965

[9] **H.-J. Zimmermann**: *Fuzzy programming and linear programming with several objective functions,* Fuzzy sets and systems, 1(1):45–55, 1978

Journal of Energy Technology

JET Volume 9 (2016) p.p. 45-56
Issue 4, December 2016
Type of article 1.04
www.fe.um.si/en/jet.html

CLEANING OF FLUE GASES IN THERMAL POWER PLANTS

ČIŠČENJE DIMNIH PLINOV V TERMOENERGETSKIH POSTROJENJIH

Martin Bricl[ℜ]

Keywords: FGD, desulphurization of flue gases, dry desulphurization process, CFB technology, semi-dry desulphurization process, SDA technology, wet calcite process.

Abstract

In the scope of this paper, all three processes for desulphurization of flue gases (FGD) are presented. These are a dry procedure, a semi-dry procedure, and a wet calcite procedure for desulphurization of flue gases. Each procedure is described, and the main chemical reactions between acid components in flue gases with reagent and schematic flow chart drawings of each desulphurization procedure are presented. The focus of this paper is to acquaint the reader with the technological possibilities for flue gas desulphurization processes.

Povzetek

V sklopu članka obravnavamo tri postrojenja za čiščenje dimnih plinov (razžvepljevanje dimnih plinov). To so suhi postopek, pol suhi postopek in mokri postopek za čiščenje dimnih plinov. Vsako postrojenje je opisano, predstavljene so osnovne kemijske reakcije procesa in shematska tehnološka risba postrojenja za odžvepljevanje dimnih plinov. Namen članka je seznaniti bralca z tehnološkimi možnostmi postrojenj za čiščenje dimnih plinov.

ℜ Corresponding author: Martin Bricl, University of Maribor, Faculty of Energy Technology, Hočevarjev trg 1, SI 8270 Krško, Tel.: +386 51 210 620, Email address: martin.bricl@student.um.si

1 INTRODUCTION

In the last decade, large thermal power plants were forced to build and improve their flue gas treatment systems, because many countries in the developed world had passed legislation dictating the level of emissions that a polluter must not exceed in order to be able to operate in the future, *[1].* The systems for flue gas treatment in thermal power plants are intended to lower acid and dust components in order to maintain the health of the environment to the greatest extent possible, *[2]*.

This paper will be focused on systems for reducing sulphur dioxide from flue gases in thermal power plants, *[3]*. All three currently commonly used desulphurization processes for flue gases (dry calcite process, semi-dry, and wet process for desulphurization of flue gases, commonly known as DeSOx processes) will be presented, *[4]*.

We will make a detailed review of the wet process for desulphurization of flue gases in thermal power plants because it is the most commonly chosen BAT, *[5],* (Best Available Technology). Its advantages are its favourable reagent and the harmlessness of cleaning the by-product, which can be further used in other parts of industry or disposed of in the environment, without any known side effects. With detailed engineering from the beginning of the desulphurization process to its execution, a very high level of scrubbing acid components from flue gases can be achieved by using a proper reagent; lime or limestone are often used. A by-product of this process is gypsum. It can be used for commercial purposes or further inside a thermal power plant as a medium in other industrial processes, such as the stabilization of electrostatic precipitator ash.

2 SULPHUR DIOXIDE

Sulphur is a chemical component and is present in every coal that is burnt in boilers to produce steam that drives turbines and generators to produce electricity. As the quality of coal can vary, so too can the amount of sulphur that is present in it. We can assume that the lower the coal quality is, the higher the amount of sulphur. As coal is burned in boilers, gaseous elements are formed: sulphur dioxides in a gaseous state. Other similarly formed components in boilers are sulphur trioxide (SO_3), hydrochloride (HCl), and hydrogen fluoride (HF), also in a gaseous state.

Sulphur dioxide is an irritant and a colourless gas with a characteristically sharp odour. It is a major pollutant, with large amounts produced in refineries, in old abandoned coal mines, and in the chemical and rubber industries. Especially large amounts of this gas are emitted through flue gases from thermal power plants, which use coal as their primary fuel.

When sulphur dioxide enters the atmosphere, it reacts with oxygen and water, and sulfuric acid is formed. This phenomenon is known as acid rain, and it affects human health and nature, especially forests. It also affects buildings and monuments, and real estate in general.

3 DRY DESULPHURIZATION PROCESS

The dry calcite process is also known as the circulating fluidized bed process or the CFB process. For the removal of acid components from flue gases, hydrated lime is used. Together with ash from the boiler, the hydrated lime is circulating inside the absorber and electrostatic precipitator. In these two devices, the entire reaction of cleaning of flue gases occurs. The system for dry cleaning of flue gases consists of absorbent storage, reagent preparation, absorber (scrubber), particulate removal (ESP), recycling, and disposal devices for the reaction products.

The CFB technology dry flue gas cleaning is primarily intended for small and medium thermal power plants, which use coal with a high concentration of sulphur as their primary fuel. In comparison to the wet flue gas cleaning process, the CFB technology is relatively favourable, and its scrubber capacity and quality are very competitive. In addition, the CFB technology can also reduce the concentration of other environmentally harmful substances, such as SO_3, HCl, HF, mercury, and heavy metals, in flue gases, *[6]*.

The CFB technology has been developed to the point that it can also be used in large thermal power plants intended for high-volume electricity production. The flue gas flow in such installations could easily exceed 1 million norm m^3/h. At this level, the technology is capable of scrubbing 98% of all acid components from flue gases. The amount of sulphur in coal can be up to 2.5% in order to reach the mentioned scrubbing efficiency of the absorber. The estimated financial investment to implement a dry desulphurization unit in a thermal power plant block with a capacity of 150 MWe is approximately €49,500,000.

3.1 Working principle of dry calcite process

The basic working principle is based on technology used for more efficient coal burning in boilers: circulated fluidized bed boilers. Flue gases that come from the boiler are directed to the lower part of the CFB reactor (also called the “absorber”), into which process water and the reagent (hydrated lime) are delivered. As flue gases exit the CFB reactor chamber, they encounter the suspension of process water, hydrated lime, and ash. As the flue gasses and suspension come into contact, a chemical reaction that eliminates the acid components from the gases occurs. The main efficiency parameter of the process of scrubbing of flue gases in the reactor is the ambient temperature.

Part of the by-product of this reaction is ash that accumulates on the bottom of the reactor. From there, it is discharged from the lower manhole of the reactor on the transportation belt, which transports ash to the final disposal place. However, it is essential to maintain the proper amount of ash in the reactor in order to ensure an optimal scrubbing process. All other particles that leave the reactor chamber in the flow of flue gases are captured inside the electrostatic precipitator. In the first fields of the precipitator, usable particles of hydrated lime and ash are collected. They are returned to the reactor in order to decrease the consumption of the reagent (hydrated lime) and to lower the costs of the consumed reagent. Parts of the ash and reagent that are too small to return to the reactor chamber pass through all the stages of the electrostatic precipitator and are deposited in the central by-product silo.

From the electrostatic precipitator, flue gases are forwarded through an ID fan into the stack. The fan is needed to balance the pressure drops that are present in the system, because of the reactor chamber and electrostatic precipitators. From there, sulphur-free flue gases enter the atmosphere.

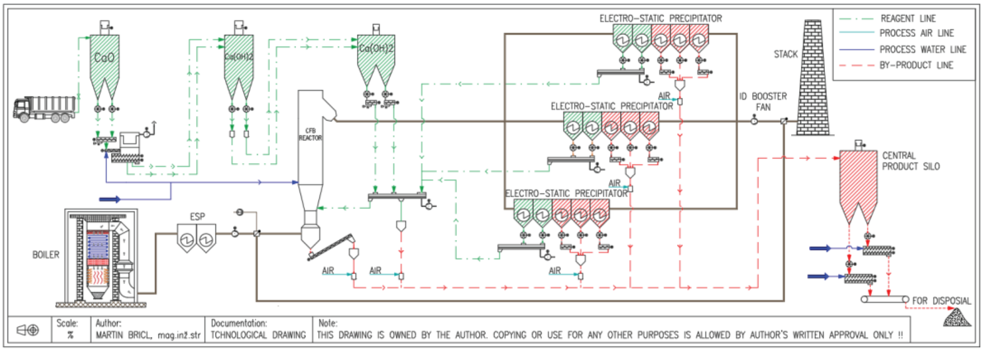

Figure 1: *Schematic technological drawing of dry desulphurization unit*

3.2 Chemical aspect of dry desulphurization process

The reaction of scrubbing acid components from flue gases happens in the reaction chamber. The reagent, which is hydrated lime $Ca(OH)_2$, ties the acid components that flue gases contain to itself. The reagent is in a liquid state, and acid components are in a gaseous state. The reagent in a liquid state is obtained from the following reaction:

$$Ca(OH)_2 + H_2O \text{ -> } Ca(OH)_2\,(aq) \leftrightarrow Ca^{2+} + 2OH^- \quad (3.01)$$

The reaction happens on the surface of hydrated lime, which has been in contact with the process water. Furthermore, flue gases need to be exposed to process water in order to achieve a high level of scrubbing process. Process water is delivered directly to the reactor chamber. The humidity of flue gases in the reactor chamber is critical. It is determined with the help of the temperature difference of flue gases before and in the reactor chamber. The optimal temperature difference is considered to be $\Delta T = 15^o C$. The main chemical reactions of the dry flue gas cleaning process are the following:

$$2\ SO_2 + 2\ Ca(OH)_2 \Rightarrow 2\ CaSO_3 \times ½\ H_2O + H_2O \quad (3.02)$$

$$2\ SO_3 + 2\ Ca(OH)_2 \Rightarrow 2\ CaSO_4 \times ½\ H_2O + H_2O \quad (3.03)$$

In the process of flue gases travelling through the reaction chamber or absorber, some other chemical reactions also take place.

$$2\ HCl + Ca(OH)_2 \Rightarrow CaCl_2 + 2\ H_2O \quad (3.04)$$

$$2\ HF + Ca(OH)_2 \Rightarrow CaF_2 + 2\ H_2O \quad (3.05)$$

As gaseous CO_2 is present in flue gases from the thermal power plant, the formation of limestone is also a part of the chemical process inside the absorber.

$$CO_2 + Ca(OH)_2 \Rightarrow CaCO_3 + H_2O \quad (3.06)$$

3.3 CFB Reactor

The CFB reactor is a steel structure consisting of five zones for flue gas cleaning, i.e. the desulphurization process. These zones are as follows:

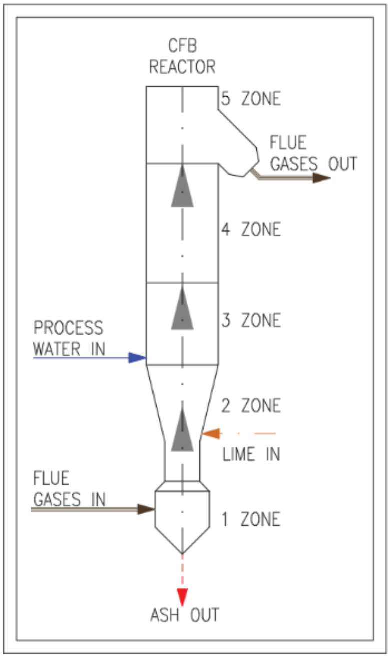

***Figure 2**: Section view of CFB reactor, where flue gases are cleaned*

- *ZONE 1: ENTRY ZONE:* Here, it is important to regulate the proper amount of volumetric flow of flue gases. If the volumetric flow is too high, there can be damage to the electrostatic precipitator.
- *ZONE 2: VENTURI ZONE*: In this section, flue gases must be accelerated to reach suitable velocity to achieve the highest efficiency of the cleaning process.
- *ZONE 3: FLUIDIZED BED ZONE:* Zone with the highest turbulence, where the absorption of acidic components in gases and maintaining the stability of the reagent recirculation take place. In this zone, process water for flue gases is injected.
- *ZONE 4: RECIRCULATION ZONE*: This zone is located in the upper part of the CFB reactor. Here, the second phase of absorption of acid components from flue gases is executed.
- *ZONE 5: OUTLET ZONE*: Directing the flow of flue gases out of the CFB reactor and forwarding them towards the electrostatic precipitator.

The CFB reactor chamber does not need any particular cleaning process or maintenance to achieve a sufficient cleaning effect. The reactor chamber is made of stainless steel, as this material choice ensures its long operational life.

4 SEMI-DRY DESULPHURIZATION PROCESS

The semi-dry process for flue gas desulphurization is based on the injection of a dry reagent in the reactor chamber. Additionally, through spray levels process water is also added. This process is called semi-dry because the entry reagent is wetted with process water, but a by-product of the desulphurization process is entirely dry ash, which is concentrated in the dust filter.

The semi-dry desulphurization process consists of the following steps: preparation of the semi-dry desulphurization unit in a thermal power plant block with a capacity of 150 MWe is approximately €51,500,000.

4.1 Working principle of semi-dry desulphurization process

This procedure of the desulphurization of flue gases is relatively simple. It consists of a reagent preparation module, an absorption chamber, and a fabric filter. Hot raw flue gases enter the absorption chamber through the flue gas disperser, where they come in contact with small drops of the previously prepared limestone suspension (average size of a suspension drop is just 50 μm). Acid components in flue gases are absorbed by alkaline components in suspension. The presence of water in the suspension drops is quickly eliminated because of the very high temperature in absorption chamber. The dynamic control of flue gas distribution, suspension production, and control of suspension drops size, ensures that there is no accumulation of water or parts of reagent inside the absorption chamber.

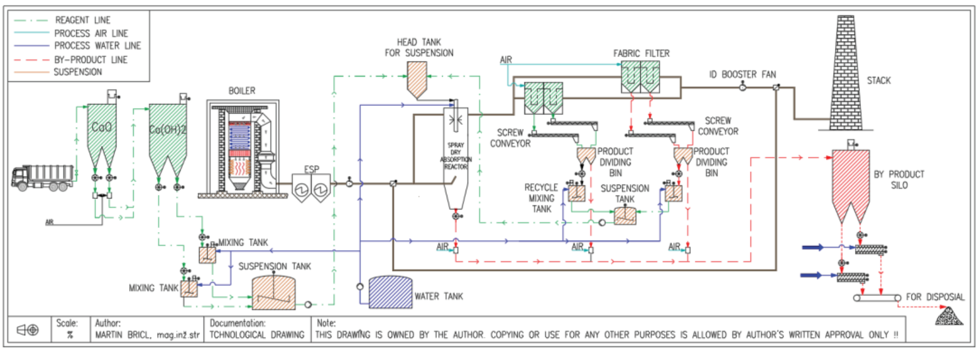

Figure 3: *Schematic technological drawing of semi-dry desulphurization unit*

A part of reagent and flue gas-ash is accumulated on the bottom of the absorption chamber, from where it is transported to the central by-product silo. Flue gases that pass through the absorption chamber are further directed to the fabric filter, where ash and dust particles are absorbed to prevent their entry into the atmosphere. Additionally, a part of unused reagent in dry form is returned to the first stage of reagent preparation in order to reduce reagent use. From fabric filter, flue gases directed to the stack, from where they enter the atmosphere, are cleaned. In order to eliminate pressure drops in the path of the flue gases, an additional ID fan needs to be integrated into flue gas ducts.

4.2 Chemical aspect of semi-dry desulphurization process

The two most important steps in the semi-dry desulphurization process are the following:

- Process of drop formation of sizes less or equal to 50 μm;
- Effective dispersion of raw flue gases to exploit the biggest exposure of raw flue gases to the reagent suspension drops.

The chemical reactions take place inside the absorption chamber. Alkaline components in suspension drops absorb acid components from the flue gases (SO_2, SO_3, HCl, and HF). The reagent used for the semi-dry process is slaked lime or calcium hydroxide. The main chemical reactions of this process are the following:

$$SO_2 + Ca(OH)_2 \Rightarrow CaSO_3 + H_2O \quad (4.01)$$

A small part of SO_2 reacts with alkaline substances as follows:

$$SO_2 + \frac{1}{2} O_2 + Ca(OH)_2 \Rightarrow CaSO_4 + H_2O \quad (4.02)$$

Most of the sulphur dioxide reacts with suspension drops while they are still in the wet phase inside the absorption chamber. After the cleaning process of raw flue gases in the chamber, they are directed to the fabric filter, which has (as mentioned before) two main important tasks. These are:

- Separation of by-product, ash, and dust particles;
- Additional absorption of acid components in flue gases.

In addition, it should be mentioned that the absorption of CO_2 is part of the semi-dry desulphurization process. However, SO_2 is much more acidic than CO_2 and is, therefore, more strongly suppressed by alkaline suspension than CO_2 is. Part of it is, however, suppressed in the absorption chamber and is prevented from exiting the atmosphere. The amount of the suppressed CO_2 is very small in comparison with SO_2. A specific feature of the semi-dry desulphurization process is the use of process water with the addition of chlorides. That positively affects the absorption process inside the absorption chamber. Instead of process water with added chlorides, seawater can be used, depending on the location of the power plant.

4.3 Description of absorption chamber

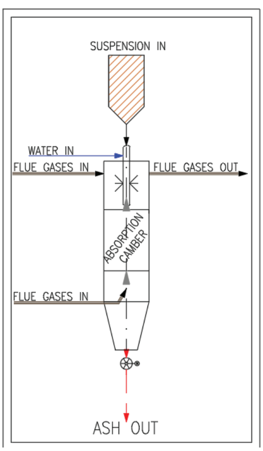

***Figure 4**: Absorption chamber of semi-dry unit*

The main component of the absorption chamber is a device to minimize suspension drops to the size of 50 µm. This is a rotary device with as corrosion- and abrasion-protected central core. The main task of this device is to distribute reagent suspension to the process. The main advantage of this device is a very quick adaptation of its operation to the changes in volumetric flue gas distribution, changes of the temperature of flue gases, or the composition of flue gases. The described unit can adapt to these changes quickly and easily; therefore, it is suitable for boilers that have changes in their operational regimes.

The chamber can process from 400,000 Nm^3/h up to 1,600,000 Nm^3/h of flue gases. In the case of a very large volumetric flow of flue gases, there can be two entrances for raw flue gases in the absorption chamber. The first entrance is on the chamber's side, where 60% of flue gases volumetric flow enters, 40% of the flue gases' volumetric flow enters through opening on the roof of the absorption chamber. The chamber is made of stainless steel. Additional inner protection of all steel surfaces against acid components is made of rubber.

5 WET DESULPHURIZATION PROCESS

The wet desulphurization process is based on a wet limestone scrubber, *[7]*. This process is commonly used in big thermal power plants, primarily because of its very high efficiency of flue gas cleaning (95–99% efficiency of scrubbing SO_2 from raw flue gases), and its very affordable reagent. The main reagent is calcite [$CaCO_3$], which is much cheaper than the lime or hydrated lime that is used as a reagent in dry and semi-dry desulphurization processes.

The end product of wet flue gas cleaning is gypsum [$CaSO_4 \times 2\ H_2O$], which can be reused in the cement and mining industries, where gypsum can be used to fill in old closed mine shafts to stabilize the mining terrain.

The main element of the wet desulphurization process is the absorber. Other parts of the equipment needed include a limestone preparation plant, where calcite or limestone is crushed and prepared in suspension. Additionally, a gypsum dewatering plant to reduce moisture in the by-product is required. Auxiliary equipment including oxidation compressors, compressors for instrumental air, high voltage electrical equipment, and pumps. In the case of emergency in the absorber, there is usually also an emergency drainage tank to empty the limestone suspension, which is located in the bottom part of the absorber.

The estimated investment to implement a wet desulphurization unit in a thermal power plant block with a capacity of 150 MWe is approximately €73,000,000, *[8]*. Because of the extensive scope of equipment, the initial investment is higher than that for the dry or semi-dry desulphurization processes. However, it should be noted that the operational costs are significantly higher for dry and semi-dry processes.

5.1 Working principle of wet desulphurization process

Raw flue gases are directed through flue gas ducts to the absorber. Fresh process water and a fresh limestone suspension are also delivered to the absorber. Fresh process water can be supplied from a nearby river or lake. Furthermore, seawater, *[9]*, is suitable for the wet desulphurization process because it contains a high amount of chlorides that improve the effect of desulphurization. The limestone suspension must be prepared in advance in the limestone preparation plant, which consists of a delivery bunker, a day silo for limestone, and wet ball mills with corresponding tanks. Limestone is crushed in the mills, particles of limestone are separated in a hydro cyclone, and suitably sized particles of limestone are passed for further suspension preparation in tanks. The suspension is delivered to the absorber from these tanks.

All chemical reactions occur in the absorber, which consists of the zones that are described in chapter 5.4 in detail. After a suitable amount of time of flue gas retention in the absorber, they exit cleansed of the SO_2 component. They enter the atmosphere through the wet stack on the absorber or through the existing stack in the thermal power plant.

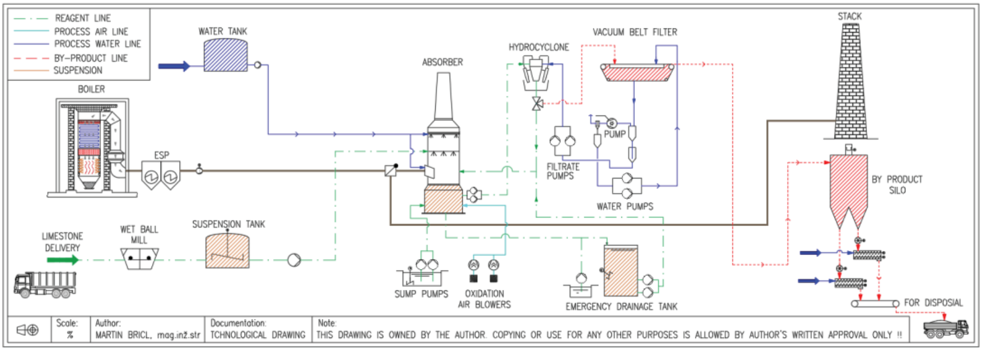

***Figure 5**: Schematic technological drawing of wet desulphurization unit*

A by-product of the wet desulphurization process is, as mentioned before, gypsum. It is pumped from the bottom of the absorber to the vacuum belt filter, where the moisture in it is eliminated. Relatively dry gypsum is then forwarded to the by-product silo and from there to the final disposal landfill. Gypsum can also be used in the cement industry, as well as a building material.

5.2 Chemical aspect of the process

The chemical aspect of the wet desulphurization process is based on reactions between the acid components in flue gases and the freshly prepared limestone suspension. The wet desulphurization process removes SO_2 from the flue gases via the absorption of acid components into the limestone suspension. A by-product of this process is gypsum. The process removes acid components, such as SO_2, SO_3, HCl, and HF, from flue gases. Some of the chemical reactions during the wet desulphurization process are summarized below.

- <u>Absorption of SO_2 into the liquid phase</u>

First, we need to achieve the conversion of sulphur dioxide from a gaseous state into a liquid state. The chemical reactions are as follows:

The acid components in flue gases, specifically Sulphur oxides SO_2, and SO_3, HCl, and HF, dissolve in water or the limestone suspension as follows:

$$SO_{2\ gaseous} \rightarrow SO_{2\ liquid} \quad (5.01)$$

$$SO_{2\ liquid} + H_2O \rightarrow H_2SO_3 \quad (5.02)$$

The next step of the wet desulphurization process is the dissociation of acid:

$$H_2SO_3 \rightarrow H^+ + HSO_3^- \quad (5.03)$$

$$H_2SO_3 \rightarrow 2H^+ + SO_3^{2-} \quad (5.04)$$

- Dissolution of limestone and neutralization reactions

Limestone dissolves in the water slurry and neutralizes acids from the flue gas absorption. A by-product of this dissolution is CO_2.

$$CaCO_{3\,(limestone)} \rightarrow CaCO_{3\,(liquid)} \quad (5.05)$$

$$CaCO_3 + H^+ \rightarrow Ca^{2+} + HCO_3^- \quad (5.06)$$

$$HCO_3^- + H^+ \rightarrow H_2O + CO_2 \quad (5.07)$$

- Oxidation reactions

The oxidized air is delivered into the lower part of the absorber through absorber agitators. It is required to oxidize the sulphite to sulphate.

$$2\ HSO_3^- + O_2 \rightarrow 2\ SO_4^{2-} + 2H^+ \quad (5.08)$$

- Crystallization and precipitation reactions

Crystallization takes place in the lower part of the absorber. The finally produced sulphate ions will react with the calcium ions. The result is the formation of gypsum.

$$Ca^{2+} + SO_4^{2-} + 2\ H_2O \leftrightarrow CaSO_4 \bullet 2\ H_2O \quad (5.09)$$

5.3 Absorber

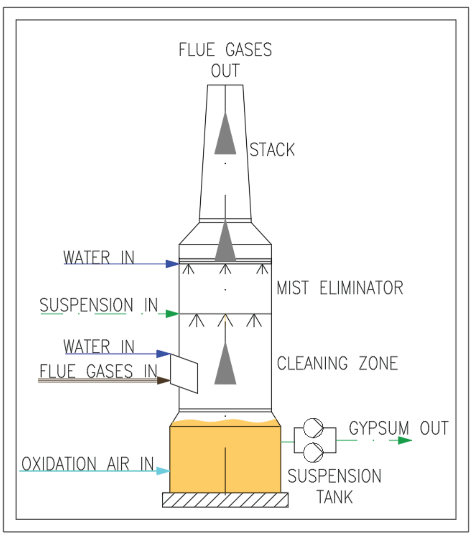

***Figure 6**: Absorber unit for wet desulphurization of raw flue gases*

As mentioned before, the absorber is the most important part of equipment in the scope of the wet desulphurization process. The wet absorber has three zones for the cleaning process. In the first zone, there is a calcite suspension tank. This suspension is then pumped with the help of circulation pumps to the spray levels, where it comes into contact with flue gases. In the second zone, the reaction is started between harmful substances in flue gases (SO_2, HCl, HF, SO_3) and the reagent in a $CaCO_3$ water suspension. As the harmful substances react with the reagent, they fall back to the bottom of the absorber where they form a by-product of wet flue gas desulphurization and cleaning: gypsum. In zone three, water drop eliminators are installed in order to return water to the process and decrease the use of process water in the cleaning process. The path of flue gases through the absorber is marked with grey arrows. The absorber must be properly technically maintained to ensure a high cleaning effect during its operational lifecycle.

6 CONCLUSION

The technology of flue gas desulphurization has its beginnings in the early 1970s. It has greatly improved the quality of living because it prevents SO_2 and other harmful substances from entering the atmosphere. Although this technology is not cheap, it has been widely implemented in almost every thermal power plant in the developed world to preserve the environment.

Further development of this technology can also be expected. All countries of the developed world have committed themselves to reducing their emissions of greenhouse gases, mainly CO_2. Pilot tests have been made on scrubbing flue gases in thermal power plants to simultaneously eliminate SO_2 and CO_2. The preliminary results have been positive, but further development of this technology and the related sorbents is required.

References

[1] **R. Jamil, L. Ming, I. Jamil, R. Jamil**: *Application and development trend of flue gas desulphurization (FGD) process: A review*, International Journal of Innovation and Applied Studies, Vol. 4, Iss. 2, p.p. 286 – 297, 2013

[2] **A. Dehghani, H. Bridjanian:** *Flue gas desulfurization methods to conserve the environment*, Petroleum & Coal, November 2010

[3] **R.K. Srivastava:** *Controlling SO_2 emissions: a review of technologies, National Risk Management Research Laboratory*, EPA/600/R-00/093, November 2000

[4] **VDI 3927 Part I:** *Waste gas cleaning – removal of sulphur oxides, nitrogen oxides and halides from combustion flue gases*, Beuth Verlag GmbH, Düsseldorf, 2000

[5] **J.B.Kitto, S.C. Stultz:** *Steam/its generation and use 41st edition*, The Babcock & Wilcox Company, Barberton, Ohio, U.S.A., 2005

[6] **P.S. Nolan:** *Flue gas desulfurization technologies for coal-fired plants*, The Babcock & Wilcox Company, Barberton, Ohio, U.S.A., November 2000

[7] **J. Oman:** *Generatorji toplote*, Univerza v Ljubljani, Fakulteta za strojništvo, Ljubljana 2005

[8] **Sergent & Lundy:** *Wet flue gas desulfurization technology evaluation*, National lime association, Chichago, U.S.A., January 2003

[9] **S. C. Christian, P. Valerin:** *Energy policies on wet flue gas desulphurization***,** Journal of Engineering Studies, vol.18, Iss. 3, 2012

Nomenclature

(Symbols)	(Symbol meaning)
FGD	Flue Gas Desulphurization
BAT	Best Available Technology
CFB	Centrifugal Fluidized Bed
SDA	Semi Dry Absorption
ID fan	Induced Draft fan
SO_2	Sulphur Dioxide
SO_3	Sulphur Trioxide
CO_2	Carbon Dioxide
HF	Hydrogen Fluoride
HCl	Hydrochloride
$CaCO_3$	Calcite
$Ca(OH)_2$	Hydrated Lime
DeSOx	Desulphurization

Journal of Energy Technology

JET Volume 9 (2016) p.p. 57-67
Issue 4, December 2016
Type of article 1.01
www.fe.um.si/en/jet.html

ANALYSIS OF THE OPPOSITE REACTIVE POWER DIRECTION PHENOMENON ON TWO PARALLEL OVERHEAD TRANSMISSION LINES

ANALIZA POJAVA NASPROTNE JALOVE MOČI NA DVEH VZPOREDNIH NADZEMNIH VODIH

Ivan Tolić[ℜ], Robert Nađ[1], Ivana Hartmann Tolić[2]

Keywords: reactive power, transmission line, measurement

Abstract

This paper presents an analysis of the opposite reactive power direction phenomenon on two parallel overhead transmission lines. Measurements are performed on transmission lines, recorded using energy meters. Superficial reasoning leads to the conclusion that the measurement system is not trustworthy. In addition, more detailed theoretical analysis shows that the phenomenon is possible and it is not the result of the incorrect measurement, but it is the result of reactive power distribution along the respective transmission lines.

Povzetek

V članku je predstavljena analiza pojava nasprotne jalove moč na dveh vzporednih nadzemnih vodih. Najprej so meritve opravljene na realnem daljnovodu in pojav je posnete z merilniki električne energije. Površno razmišljanje nas pripelje do zaključka, da je sistem merjenja dvomljiva.

ℜ Corresponding author: Ivan Tolić, Croatian Transmission System Operator Ltd., Measurement Department, Kupska 4, 10000 Zagreb, Tel.: +385 91 217 7128, E-mail address: Ivan.Tolic@hops.hr

[1] Croatian Transmission System Operator Ltd., Measurement Department, Kupska 4, 10000 Zagreb

[2] Faculty of Electrical Engineering, Computer Science and Information Technology Osijek, Department of Software Engineering, Kneza Trpimira 2B, HR-31000 Osijek

Podrobnejša teoretična analiza pa pokaže, da je ta pojav mogoč in ni posledica nepravilnega merjenja. Vendar je rezultat porazdelitve jalove moči vzdolž posameznih prenosnih vodov.

1 INTRODUCTION

In current power systems, transmission system operators (TSO) are associated with larger organizations in order to satisfy increasing requirements for energy exchange in the competitive market environment. TSOs in Europe are joined to the *European Network of Transmission System Operators for electricity* (ENTSO-E), *[1]*, where the rights and obligations are defined according to REGULATION (EC) No 714/2009 OF THE EUROPEAN PARLIAMENT AND OF THE COUNCIL, *[2]*. Transmission lines are one of the key unique components of electricity transmission, *[3]*. The rapidly increasing needs for technical and economic compromises in the competitive market environment emphasizes the importance of accurate energy measurements. Therefore, metering points are equipped with modern equipment (accuracy class 0.2) in order to meet all requirements for reliable and accurate measurement, which is the fundamental requirement for the functioning of the TSO in the above-mentioned market environment, *[4].*

2 THE DESCRIPTION OF OPPOSITE REACTIVE POWER DIRECTION PHENOMENON

2.1 The architecture of metering point

Current metering points in the high voltage power system consist of instrument transformers (voltage and current), an energy meter, and connection equipment (see Fig. 1.). The purpose of the metering point is to provide information about the measurand (measured value, i.e. the quantity of interest), *[5, 6]*.

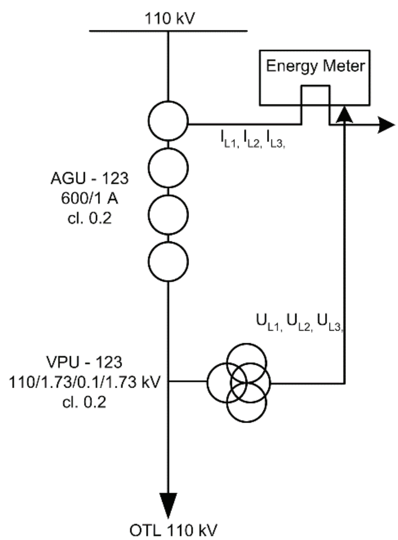

Figure 1: *The principal scheme of metering point*

For more details about the requirements for the instrument transformers and energy meters, the reader is referred to *[7–10]*.

In this paper, two parallel 110 kV overhead transmission lines (OTL) are observed (see Fig. 2). Both lines have their own independent metering point, as presented in Fig. 1.

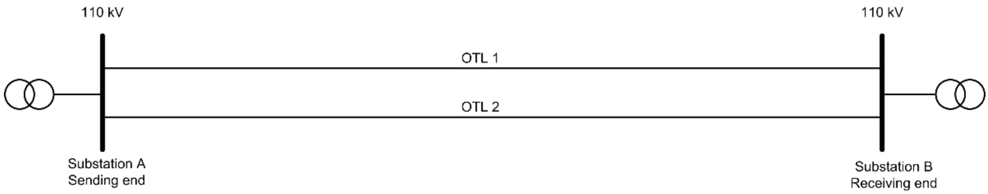

Figure 2: *Two parallel 110 kV overhead transmission lines*

Energy meters, such those as described in *[11, 12]*, measure active and reactive power and energy in two directions. In some measuring periods, the opposite reactive power direction is measured. At first glance, this phenomenon sounds ambiguous. Superficial reasoning leads to the conclusion that the quality of the measurement system is doubtful. However, more detailed analysis is necessary. Additional testing shows the correctness of the measuring system components, and the efforts are directed to an analysis of the electrical conditions on the OTL.

2.2 Measurement results

The measurement was performed on a real transmission line under the jurisdiction of the Croatian Transmission System Operator in the period of 2016/10/20 from 00:00–24:00 h. Owing to confidentiality, we are not able to publish the name of the transmission line.

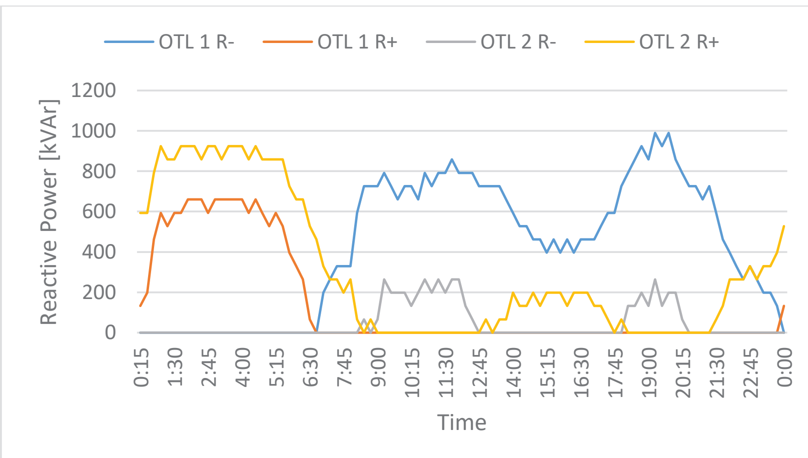

Figure 3: *Measurement results*

Fig. 3 shows the measurement results with the resolution of 15 minutes. In the periods of 6:45–8:00 h and 12:45–18:00 h the reactive powers on OTL 1 and OTL 2 are of the opposite directions, i.e. the opposite reactive power phenomenon is present. In addition, the latter phenomenon would be theoretically analysed and proofed.

3 MATHEMATICAL ANALYSIS OF THE OPPOSITE REACTIVE POWER PHENOMENON

3.1 Theoretical analysis of parallel transmission line electrical conditions

The short transmission line model, as recommended in *[14]*, is used (see Fig 4). OTL parameters are substituted using direct impedance, i.e. using its resistance *R*, inductance *L* and capacitance *C*, *[15]*.

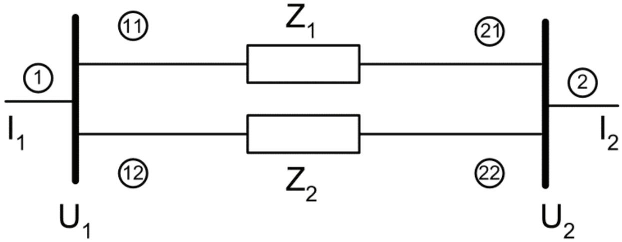

Figure 4: *Equivalent circuit of two parallel 110 kV overhead transmission lines*

Primary OTL parameters are: l_1, l_2 – line length, Z_1, Z_2 – impedances, Y_1, Y_2 – admittances, R_1, R_2 – resistances, L_1, L_2 – inductances and C_1, C_2 – capacitances. Electrical conditions are described using the following quantities: *U* – voltage, *I* – current, *S* – apparent power, *P* – active power and *Q* – reactive power. The indices that would be associated with the respective quantities are: 1 – sending end, 2 – receiving end, i.e. 11 – sending end of the first line, 21 – receiving end of the first line, 12 – sending end of the second line and 22 – receiving end of the second line (see. Fig. 4).

Owing to the calculation correctness, very small (almost negligible) capacitances to the ground should be considered in the calculation procedure. Equivalent impedances in phasor expression are calculated as (3.1) an (3.2)

$$\overline{Z_1} = R_{11}l_1 + j\omega L_{11}l_1, \tag{3.1}$$

$$\overline{Z_2} = R_{12}l_2 + j\omega L_{12}l_2. \tag{3.2}$$

Equivalent admittances are calculated as (3.3) and (3.4)

$$\overline{Y_1} = j\omega C_1, \tag{3.3}$$

$$\overline{Y_2} = j\omega C_2. \tag{3.4}$$

The total equivalent impedance is (3.5)

$$\bar{Z} = \frac{\overline{Z_1 Z_2}}{\overline{Z_1} + \overline{Z_2}}. \tag{3.5}$$

The total equivalent admittance is (3.6)

$$\bar{Y} = \bar{Y_1} + \bar{Y_2}. \tag{3.6}$$

Characteristic impedance of the OTL is (3.7)

$$\bar{Z_C} = \sqrt{\frac{\bar{Z}}{\bar{Y}}}. \tag{3.7}$$

Propagation equation for the entire line length is (3.8)

$$\bar{\Theta} = \bar{\gamma} * l = \alpha + j\beta, \tag{3.8}$$

where α is the attenuation (loss) factor, β is the phase (velocity) factor and $\bar{\gamma}$ is propagation constant, *[13]*. Transmission equations in hyperbolic form, *[16]*, with known conditions at the receiving end of the line (current, voltage) are (3.9) and (3.10)

$$\bar{V_1} = \bar{V_2} * \mathrm{ch}(\bar{\gamma} * l) + \overline{Z_C} * \bar{I_2} * \mathrm{sh}(\bar{\gamma} * l), \tag{3.9}$$

$$\bar{I_1} = \bar{I_2} * \mathrm{ch}(\bar{\gamma} * l) + \frac{\bar{V_2}}{\bar{Z_C}} * \bar{I_2} * \mathrm{sh}(\bar{\gamma} * l). \tag{3.10}$$

With the aim of calculating voltage $\bar{V_1}$ and current $\bar{I_1}$ at the sending end of the line, $sh(\bar{\gamma} \cdot l)$ and $ch(\bar{\gamma} \cdot l)$ components are calculated using (3.11) an (3.12)

$$\mathrm{sh}(\bar{\gamma} \cdot l) = \mathrm{sh}\alpha * \cos\beta + j\,\mathrm{ch}\,\alpha * \sin\beta, \tag{3.11}$$

$$\mathrm{ch}(\bar{\gamma} \cdot l) = \mathrm{ch}\alpha * \cos\beta + j\,\mathrm{sh}\,\alpha * \sin\beta, \tag{3.12}$$

and current $\bar{I_2}$ at the receiving end of the line is calculated considering the respective conditions (power and voltage) (3.13)

$$\bar{I_2} = \frac{P_2{}^{\angle -\varphi}}{\sqrt{3}U_2 cos^{\varphi}}. \tag{3.13}$$

The above-mentioned values describe the conditions at the ends of the line for two parallel lines together. Hence, the respective conditions for both lines individually are to be calculated. From Kirchhoff currents law applied at the sending end of the line follows by (3.14)

$$\bar{I_1} = \overline{I_{11}} + \overline{I_{12}} \xrightarrow{yields} \overline{I_{12}} = \bar{I_1} - \overline{I_{11}}. \tag{3.14}$$

The lines are connected in parallel, and thus the voltages are equal (3.15) and (3.16)

$$\overline{I_{11}} * \overline{Z_1} = \overline{I_{12}} * \overline{Z_2}, \tag{3.15}$$

$$\overline{I_{11}} * \overline{Z_1} = (\bar{I_1} - \overline{I_{11}}) * \overline{Z_2}. \tag{3.16}$$

From (3.16) follows the current $\overline{I_{11}}$ at the sending end of the first line by (3.17)

$$\overline{I_{11}} = \frac{\bar{I_1}\overline{Z_2}}{\overline{Z_1}+\overline{Z_2}}. \tag{3.17}$$

From (3.14) and (3.17) follows the current $\overline{I_{12}}$ at the sending end of the second line. The apparent powers $\overline{S_{11}}$ and $\overline{S_{12}}$ at the sending ends of the lines are calculated as (3.19)

$$\overline{S_{11}} = 3\bar{V_1}\overline{I_{11}}, \tag{3.18}$$

and (3.19)

$$\overline{S_{12}} = 3\bar{V_1}\overline{I_{12}}. \tag{3.19}$$

From Kirchhoff currents law applied at the receiving end of the line, follows (3.20)

$$\overline{I_2} = \overline{I_{21}} + \overline{I_{22}} \xrightarrow{yields} \overline{I_{22}} = \overline{I_2} - \overline{I_{21}}. \quad (3.20)$$

The lines are connected parallel, and thus the voltages are equal by (3.21) and (3.22)

$$\overline{I_{21}} * \overline{Z_1} = \overline{I_{22}} * \overline{Z_2}, \quad (3.21)$$

$$\overline{I_{21}} * \overline{Z_1} = (\overline{I_2} - \overline{I_{21}}) * \overline{Z_2}. \quad (3.22)$$

From (3.22) follows the current $\overline{I_{21}}$ at the receiving end of the first line (3.23)

$$\overline{I_{21}} = \frac{\overline{I_2}\,\overline{Z_2}}{\overline{Z_1} + \overline{Z_2}}. \quad (3.23)$$

From (3.20) and (3.23) follows the current $\overline{I_{22}}$ at the receiving end of the second line. The apparent powers $\overline{S_{21}}$ and $\overline{S_{22}}$ at the sending ends of the lines are calculated as (3.24)

$$\overline{S_{21}} = 3\overline{V_2}\,\overline{I_{21}}, \quad (3.24)$$

and (3.25)

$$\overline{S_{22}} = 3\overline{V_2}\,\overline{I_{22}}. \quad (3.25)$$

3.2 Numerical proof of the opposite reactive power phenomenon

Owing to confidentiality, we are not able to publish the names of the OTLs, but the measurement results are from a real transmission system. Primary parameters of the OTLs are presented in Table 1.

Table 1: *Primary parameters of OTLs*

Parameter	OTL 1	OTL 2
Line length *l*, [km]	4.95	5.64
Resistance *R*, [Ω/km]	0.1388	0.1946
Inductance *L*, [mH/km]	1.3111	1.3528
Capacitance *C*, [nF/km]	8.8872	8.5944

The electrical conditions considered for the purposes of a numerical example are at the moment the opposite reactive powers measured using energy meters. The calculation procedure is started for measured quantities at the receiving end of the OTL: $\overline{U_2} = 110^{\angle 0^\circ}$ kV (line voltage) and $\overline{S_2} = P_2 + jQ_2 = 30 + j2$ MVA.
Other needed OTL parameters are calculated using equations (3.1) – (3.12), and the results are presented in Table 2.

Table 2: *Calculated parameters of OTLs*

Parameter	OTL 1	OTL 2
Equivalent impedance [Ω]	$2.150^{\angle 71.38^\circ}$	$2.630^{\angle 65.33^\circ}$
Total impedance $\bar{Z}$ [Ω]	$1.180^{\angle 68.6^\circ}$	
Equivalent admittance [S]	$j1.382*10^{-5}$	$j1.523*10^{-5}$
Total admittance $\bar{Y}$ [S]	$j2.905*10^{-5}$	
Characteristic impedance $\bar{Z}_C$ [Ω]	$201.543^{\angle -10.47^\circ}$	
Propagation constant $\bar{\Theta}$	$1.087*10^{-3} + j5.753*10^{-3}$	
Attenuation (loss) factor *α*	$1.087*10^{-3}$	
Phase (velocity) factor *β*	$5.753*10^{-3}$	
$\mathrm{sh}(\bar{\gamma} \cdot l)$	$5.855 * 10^{-3\angle 72.3^\circ}$	
$\mathrm{ch}(\bar{\gamma} \cdot l)$	$0.999^{\angle 0^\circ}$	

Calculation results for the electrical parameters for both OTLs together are presented in Table 3.

Table 3: *Electrical parameters of both OTLs together*

Parameter	Sending end	Receiving end
Line voltage *U*, [kV]	$110.161^{\angle 0.14^\circ}$	$110^{\angle 0^\circ}$
Current *I*, [A]	$157.900^{\angle -3.1^\circ}$	$157.810^{\angle -3.81^\circ}$
cosρ	0.9984	0.9978
Apparent power $\bar{S}$, [MVA]	$30.128^{\angle 3.24^\circ}$	$30.066^{\angle 3.81^\circ}$

Calculation results for the electrical parameters for both OTLs separately are presented in Table 4.

Table 4: *Electrical parameters of both OTLs separately*

Parameter	Sending end		Receiving end	
	OTL 1	OTL2	OTL 1	OTL2
Current *I*, [A]	$87.060^{\angle -5.87^\circ}$	$71.061^{\angle 0.29^\circ}$	$87.01^{\angle -6.58^\circ}$	$71.02^{\angle -0.42^\circ}$
Apparent power $\bar{S}$, [MVA]	$16.610^{\angle 6.00^\circ}$	$13.560^{\angle -0.148^\circ}$	$16.578^{\angle 6.58^\circ}$	$13.530^{\angle -0.42^\circ}$
Active power *P*, [MW]	16.520	13.560	16.468	13.530
Reactive power *Q*, [MVAr]	**1.736**	**-0.035**	1.899	0.099

From the results, it can be observed that the reactive powers $Q_{11} = 1.736\ \mathrm{MVAr}$ (sending end of a first OTL) and $Q_{12} = -0.035\ \mathrm{MVAr}$ (receiving end of a second OTL) are of the opposite signs. Therefore, the mathematical calculation shows that opposite directions of the reactive power on two parallel OTLs is theoretically possible.

3.3 Physical interpretation of the results

From the point of view of the transmission network, receiving end acts as a consumer of inductive reactive power. Let us consider the sending end to be a referent point for the calculation of energy directions. In this case, the direction of reactive power "R-" means that the sending end sends inductive reactive power while direction "R+" conversely means that the sending end receives inductive reactive power. In the described phenomenon that occurs in certain periods, the sending end in one OTL receives and the second OTL gives the reactive power. Therefore, the reactive powers are in mutually opposite directions. Since the OTLs are relatively short (ca. 5 km) and their capacity against the ground is very small (the contribution of reactive power is about 100 kVAr per OTL), it is to be assumed that the cause of the phenomenon is not in the capacity of the OTLs. This is what makes the phenomenon confused, and at the first moment, the validity of measurements was doubtful. The detailed analysis of the phenomenon leads to an entirely different result. Fig. 5. shows the phasors of the voltage and currents at the sending end of the OTL.

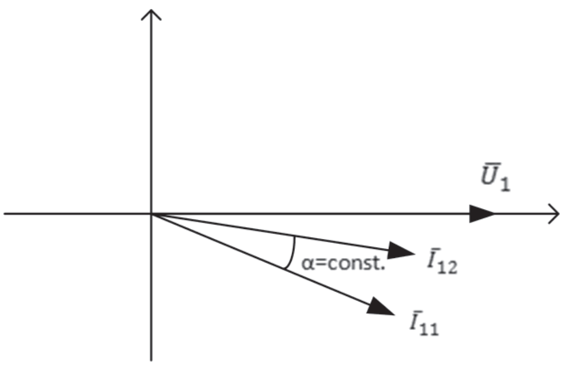

Figure 5: *Currents and voltage at the sending end of the OTL*

It is worth noting that the angle between the currents is independent of load. By changing the load, the angle of current to voltage is proportionally changed. By increasing the load, the angle increases, i.e. approaching the voltage and in the respective moment will cross over. Such an operating condition is shown in Fig. 6.

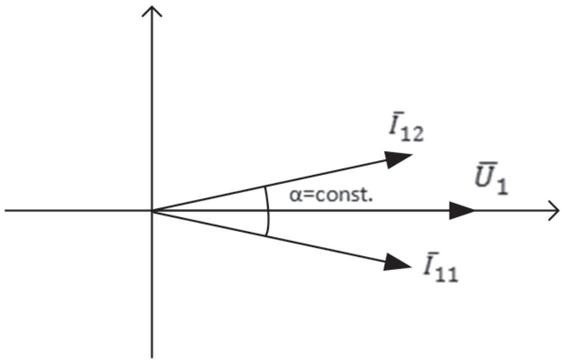

Figure 6: *Currents and voltage at the sending end of the OTL during the opposite reactive power phenomenon*

It is clear that the reactive powers are in the opposite directions. Energy meters register this as the sending end while simultaneously receiving reactive power on one OTL and sending reactive power on the other OTL. From the physical and mathematical point of view, it is obvious that the presented operating condition can be explained independently of the capacity against the ground. This confirms that the reason for the presented phenomenon is not the distribution of capacitive currents along the lines nor incorrect measurement, but this phenomenon comes only due to the distribution of reactive powers along the impedances of the respective OTLs.

4 CONCLUSION

This paper presents an analysis of the opposite reactive power direction on two parallel overhead transmission lines. At the first, the latter phenomenon was measured on the real transmission line using energy meters and seemed ambiguous, i.e. superficial reasoning leads to the conclusion that the quality of the measurement system is doubtful. Additional theoretical analysis was performed. The results show that the phenomenon is theoretically possible and it is independent of the capacities against the ground. Moreover, it is not the result of the incorrect measurement, but it originates only due to the distribution of the reactive powers along the impedances of the transmission lines.

References

[1] **'European network of transmission system operators for electricity'**, https://www.entsoe.eu/Pages/default.aspx, accessed April 2016

[2] **The European Commission:** *Regulation (EC) No 714/2009 - on conditions for access to the network for cross-border exchanges in electricity and repealing Regulation* (EC), No. 1228/2003 (2009)

[3] **L. Jozsa:** *Nadzemni vodovi,* Faculty of Electrical Engineering in Osijek, 2011

[4] **T. Gonen:** *Electric Power Transmission-System Engineering*, John Wiley & Sons, 1988

[5] **Ž. Modrić, Z. Kovač, K. Fekete:** *Determination of Energy Interchanged on the Tie Lines—Some Practical Issues*, Journal of Energy and Power Engineering, 2014, iss. 8, pp. 948–956

[6] **JCGM:** *Evaluation of measurement data — Supplement 1 to the "Guide to the expression of uncertainty in measurement" — Propagation of distributions using a Monte Carlo method*, 2008

[7] **IEC 60044-1:1996 Instrument transformers - Part 1**: *Current transformers*, https://webstore.iec.ch/publication/12389, accessed October 2016

[8] **IEC 61869-2:2012 Instrument transformers - Part 2:** *Additional requirements for current transformers*, https://webstore.iec.ch/publication/6050, accessed October 2016

[9] **IEC 61869-3:2011 - Part 3:** A*dditional requirements for inductive voltage transformers*, https://webstore.iec.ch/publication/6051, accessed October 2016

[10] **IEC 62053-22:2003 Electricity metering equipment (a.c.) - Particular Requirements - Part 22:** *Static meters for active energy (classes 0,2 S and 0,5 S)*, https://webstore.iec.ch/publication/6383, accessed October 2016

[11] **Landes&Gyr AG:** *High Precision Metering ZMQ202/ZFQ202 User Manual,* 2005

[12] **ISKRAEMECO:** *Three-phase electronic multi-function meter for industry - Technical Description*, 2013

[13] **D. F. Wiliams, R. B. Marks:** *Transmission Line Capacitance Measurement*, IEEE Microwave and Guided Wave Letters, 1991, vol. 1, iss. 9, pp. 243–245

[15] **M. N. O. Sadiku, L. C. Agba:** *A Simple Introduction to the Transmission-Line Modeling*, IEEE Transactions on Circuits and Systems, 1990, vol. 37, iss. 8, pp. 991–999

[16] **G. Sivanagaraju, S. Chakrabarti, S. C. Srivastava:** *Uncertainty in Transmission Line Parameters*: *Estimation and Impact on Line Current Differential Protection*, *IEEE Trans. Instrum. Meas.*, 2014, vol. 63, iss. 6, pp. 1496–1504

MAIN TITLE OF THE PAPER SLOVENIAN TITLE

Author[1], Author [2], Corresponding author[ℜ]

Keywords: (Up to 10 keywords)

Abstract

Abstract should be up to 500 words long, with no pictures, photos, equations, tables, only text.

Povzetek

(Abstract in Slovenian language)

Submission of Manuscripts: All manuscripts must be submitted in English by e-mail to the editorial office at jet@um.si to ensure fast processing. Instructions for authors are also available online at http://www.fe.um.si/en/jet/author-instructions.html.

Preparation of manuscripts: Manuscripts must be typed in English in prescribed journal form (MS Word editor). A MS Word template is available at the Journal Home page.

A title page consists of the main title in the English and Slovenian language; the author(s) name(s) as well as the address, affiliation, E-mail address, telephone and fax numbers of author(s). Corresponding author must be indicated.

Main title: should be centred and written with capital letters (ARIAL bold 18 pt), in first paragraph in English language, in second paragraph in Slovenian language.

Key words: A list of 3 up to 6 key words is essential for indexing purposes. (CALIBRI 10pt)

Abstract: Abstract should be up to 500 words long, with no pictures, photos, equations, tables, - text only.

Povzetek: - Abstract in Slovenian language.

Main text should be structured logically in chapters, sections and sub-sections. Type of letters is Calibri, 10pt, full justified.

ℜ Corresponding author: Title, Name and Surname, Organisation, Department, Address, Tel.: +XXX x xxx xxx, E-mail address: x.x@xxx.xx

[1] Organisation, Department, Address

[2] Organisation, Department, Address

Units and abbreviations: Required are SI units. Abbreviations must be given in text when first mentioned.

Proofreading: The proof will be send by e-mail to the corresponding author in MS Word's Track changes function. Corresponding author is required to make their proof corrections with accepting or rejecting the tracked changes in document and answer all open comments of proof reader. The corresponding author is responsible to introduce corrections of data in the paper. The Editors are not responsible for damage or loss of submitted text. Contributors are advised to keep copies of their texts, illustrations and all other materials.

The statements, opinions and data contained in this publication are solely those of the individual authors and not of the publisher and the Editors. Neither the publisher nor the Editors can accept any legal responsibility for errors that could appear during the process.

Copyright: Submissions of a publication article implies transfer of the copyright from the author(s) to the publisher upon acceptance of the paper. Accepted papers become the permanent property of "Journal of Energy Technology". All articles published in this journal are protected by copyright, which covers the exclusive rights to reproduce and distribute the article as well as all translation rights. No material can be published without written permission of the publisher.

Chapter examples:

1 MAIN CHAPTER

(Arial bold, 12pt, after paragraph 6pt space)

1.1 Section

(Arial bold, 11pt, after paragraph 6pt space)

1.1.1 Sub-section

(Arial bold, 10pt, after paragraph 6pt space)

Example of Equation (lined 2 cm from left margin, equation number in normal brackets (section. equation number), lined right margin, paragraph space 6pt before in after line):

Equation (1.1)

Tables should have a legend that includes the title of the table at the top of the table. Each table should be cited in the text.

Table legend example:

Table 1: *Name of the table (centred, on top of the table)*

Figures and images should be labelled sequentially numbered (Arabic numbers) and cited in the text – Fig.1 or Figure 1. The legend should be below the image, picture, photo or drawing.

Figure legend example:

Figure 1: *Name of the figure (centred, on bottom of figure, photo, or drawing)*

References

[1] **N. Surname:** *Title,* Journal Title, Vol., Iss., p.p., Year of Publication

[2] **N. Surname:** *Title,* Publisher, Year of Publication

[3] **N. Surname:** *Title* [online], Publisher or Journal Title, Vol., Iss., p.p., Year of Publication. Available: website (date accessed)

Examples:

[1] **J. Usenik**: *Mathematical model of the power supply system control*, Journal of Energy Technology, Vol. 2, Iss. 3, p.p. 29 – 46, 2009

[2] **J. J. DiStefano, A.R. Stubberud, I. J. Williams**: *Theory and Problems of Feedback and Control Systems*, McGraw-Hill Book Company, 1987

[3] **T. Žagar, L. Kegel:** *Preparation of National programme for SF and RW management taking into account the possible future evolution of ERDO* [online], Journal of Energy Technology, Vol. 9, Iss. 1, p.p. 39 – 50, 2016. Available: http://www.fe.um.si/images/jet /Volume 9_Issue1/03-JET_marec_2016-PREPARATION_OF_NATIONAL.pdf (7. 10. 2016)

Example of reference-1 citation: In text *[1],* text continue.

Nomenclature

(Symbols)	(Symbol meaning)
t	time

JET

JET | Journal of Energy Technology | Vol. 9, Issue 3, December 2016 | University of Maribor, Faculty of Energy Technology

ISSN 1855-5748

9 771855 574008